3

Linear elasticity solutions

The equations of linear elasticity are derived in chapters 1 and 2, and can be divided into three groups: the equilibrium equations, the strain displacement equations, and the constitutive laws. Figure 3.1 shows these three groups of equations in a block diagram.

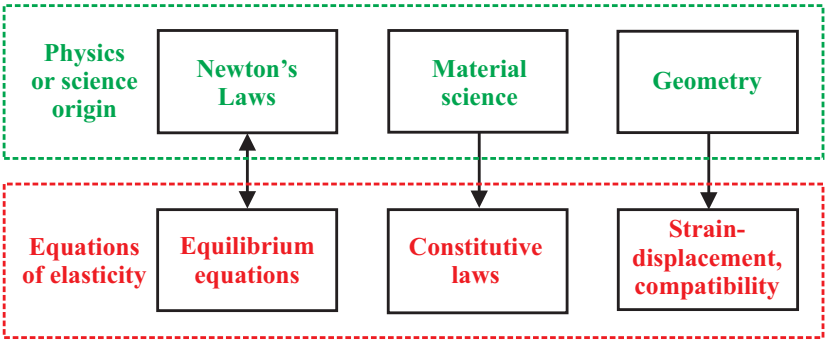

Fig. 3.1. The elasticity equations separated into three groups.

The *equilibrium equations* express the equilibrium conditions for a differential element of the body in terms of the stress field. These equilibrium conditions are a direct consequence Newton's laws applied to a differential element of the deformable body. They consists of the three partial differential equations of equilibrium, eqs. (1.4).

The *strain-displacement equations*, also called the *kinematic equations*, describe the deformation of the body without reference to the forces that create the deformation. The strain components are defined based on a purely kinematic description of the deformed and undeformed configurations of the solid. The strain-displacement equations consists of the six partial differential equations relating the strain components to the displacement components, eqs. (1.63) and (1.71).

The *constitutive laws* describe the behavior of materials under load. More specifically, they take the form of relationships linking the stress and strain components at a point. Constitutive laws are rooted in material science and express an approximation to the observed behavior of actual materials. For Hooke's law, they consists of six algebraic equations, eqs. (2.4) and (2.9).

A total of 15 equations of linear elasticity are obtained. Given the proper boundary conditions, these 15 equations can be solved to obtain the following 15 unknowns: the three components of the displacement vector, the six components of the strain tensor, and the six components of the stress tensor.

In addition, the six partial differential strain compatibility equations, eqs. (1.106), impose certain continuity conditions on the displacement components that may arise from a state of strain. While these compatibility equations are not part of the basic 15 equations of elasticity, their use may be a critical element of any solution procedure. In this chapter, solutions of this set of equations will be presented for very simple problems. Indeed, exact solutions for realistic problems are very difficult to obtain in general.

3.1 Solution procedures

The linear equations of elasticity form a set of coupled partial differential equations that are elegantly simple but like most partial differential equations, are often quite difficult to solve for realistic problems. Considerable simplification can be achieved when the general, three-dimensional formulation is reduced to a two-dimensional formulation by assuming the problem to be either plane stress or plane strain, as discussed in sections 1.3 or 1.6, respectively. Further simplification can be achieved for problems presenting specific symmetries. For example, the governing equations for two-dimensional problems featuring cylindrical symmetry reduce to ordinary differential equations. It is often necessary, however, to reformulate the elasticity equations in cylindrical or spherical coordinates to take advantage of specific symmetries or easily impose boundary conditions.

Three approaches are available for the solution of elasticity problems.

1. *Displacement formulations:* the objective is to derive three equations for the three unknown displacement components.
2. *Stress formulations:* the objective is to solve for the state of stress in the body. This means that six equations are required for the six stress components.
3. *Semi-inverse approaches:* assumptions are made to solve the problem for a subset of the variables. With that solution at hand, the remaining equations of the problem are solved. If all equations can be exactly satisfied, an exact solution is obtained and the initial assumptions are validated.

For all three approaches, dimensional reduction is often performed first. Under specific conditions, the initial three-dimensional problem can be reduced to a two- and sometimes one-dimensional problem, considerably easing the solution process. Examples of these various approaches are given in the following sections.

3.1.1 Displacement formulation

A formulation leading to equations involving only the displacement components, u_1, u_2, and u_3, is readily developed based on the following procedure.

1. Substitute the stress-strain equations (2.4) and (2.9) into the three equilibrium equations (1.4) to obtain three equations expressed in terms of strain components.
2. Substitute the strain-displacement equations (1.63) and (1.71) into these equations to obtain a set of three equilibrium equations expressed in terms of the displacement components, u_1, u_2, and u_3 alone.

These equations are generally referred to as *Navier's equations*. Given appropriate boundary conditions expressed in terms of displacement components, solution of Navier's equations yields the unknown displacement field throughout the body. While specification of displacement boundary conditions is straightforward, the specification of traction boundary conditions in terms of displacements often lead to complicated formulations. It is left as an exercise to show that Navier's equations are

$$\frac{E}{2(1+\nu)(1-2\nu)}\frac{\partial e}{\partial x_1} + G\,\nabla^2 u_1 + b_1 = 0 \tag{3.1a}$$

$$\frac{E}{2(1+\nu)(1-2\nu)}\frac{\partial e}{\partial x_2} + G\,\nabla^2 u_2 + b_2 = 0 \tag{3.1b}$$

$$\frac{E}{2(1+\nu)(1-2\nu)}\frac{\partial e}{\partial x_3} + G\,\nabla^2 u_3 + b_3 = 0, \tag{3.1c}$$

where e is the volumetric strain defined by eq. (1.75). The differential operator, ∇^2, called the *Laplacian*, is defined as

$$\nabla^2 = \frac{\partial^2}{\partial x_1^2} + \frac{\partial^2}{\partial x_2^2} + \frac{\partial^2}{\partial x_3^2}. \tag{3.2}$$

If body forces are constant throughout the body, taking a derivative with respect to x_1, x_2, and x_3 of eqs. (3.1a), (3.1b) and (3.1c), respectively, and summing up the resulting equations leads to

$$\frac{\partial e}{\partial x_1^2} + \frac{\partial e}{\partial x_2^2} + \frac{\partial e}{\partial x_3^2} = \nabla^2 e = 0. \tag{3.3}$$

Thus, for constant body forces, the volumetric strain satisfies the homogeneous Laplace's equation.

3.1.2 Stress formulation

It is a much more difficult task to formulate elasticity equations in terms of the stress components. The three equilibrium equations alone are not sufficient to determine

the six unknown stress components. In this case, the compatibility equations must be included to insure that stress components correspond to a deformation state that is continuous and sufficiently smooth. The formulation is quite tedious but can be accomplished by following the steps.

1. Substitute the stress-strain equations (2.4) and (2.9) into the six compatibility equations (1.106).
2. Further simplify these six equations into three equations for the normal stresses and three equations for the shear stresses.

The resulting equations are called *Beltrami-Michell's equations*, which can be written as

$$\nabla^2\sigma_1 + \frac{1}{1+\nu}\frac{\partial^2 I_1}{\partial x_1^2} + \frac{\nu}{1-\nu}\left(\frac{\partial b_1}{\partial x_1} + \frac{\partial b_2}{\partial x_2} + \frac{\partial b_3}{\partial x_3}\right) + 2\frac{\partial b_1}{\partial x_1} = 0, \tag{3.4a}$$

$$\nabla^2\sigma_2 + \frac{1}{1+\nu}\frac{\partial^2 I_1}{\partial x_2^2} + \frac{\nu}{1-\nu}\left(\frac{\partial b_1}{\partial x_1} + \frac{\partial b_2}{\partial x_2} + \frac{\partial b_3}{\partial x_3}\right) + 2\frac{\partial b_1}{\partial x_2} = 0, \tag{3.4b}$$

$$\nabla^2\sigma_3 + \frac{1}{1+\nu}\frac{\partial^2 I_1}{\partial x_3^2} + \frac{\nu}{1-\nu}\left(\frac{\partial b_1}{\partial x_1} + \frac{\partial b_2}{\partial x_2} + \frac{\partial b_3}{\partial x_3}\right) + 2\frac{\partial b_1}{\partial x_3} = 0, \tag{3.4c}$$

$$\nabla^2\tau_{12} + \frac{1}{1+\nu}\frac{\partial^2 I_1}{\partial x_1 \partial x_2} + \left(\frac{\partial b_1}{\partial x_2} + \frac{\partial b_2}{\partial x_1}\right) = 0, \tag{3.4d}$$

$$\nabla^2\tau_{23} + \frac{1}{1+\nu}\frac{\partial^2 I_1}{\partial x_2 \partial x_3} + \left(\frac{\partial b_2}{\partial x_3} + \frac{\partial b_3}{\partial x_2}\right) = 0, \tag{3.4e}$$

$$\nabla^2\tau_{31} + \frac{1}{1+\nu}\frac{\partial^2 I_1}{\partial x_3 \partial x_1} + \left(\frac{\partial b_1}{\partial x_3} + \frac{\partial b_3}{\partial x_1}\right) = 0, \tag{3.4f}$$

where I_1 is the first stress invariant given by eq. (1.15a). These equations, along with appropriate stress boundary conditions, can be solved for the stress state within the body. Solutions to all but the simplest problems are extremely difficult to construct. Moreover, many problems of practical interest involve boundary conditions expressed in terms of displacement components over parts of the body and in terms of stress components over other portions of the body; this leads to so called "mixed boundary value problems," which are very difficult to handle for all but the simplest problems.

If body forces are constant throughout the body, summing up eqs. (3.4a) to (3.4c) leads to $\nabla^2 I_1 = 0$, *i.e.*, the first stress invariant satisfies the homogeneous Laplace's equation. Introducing eq. (2.18), this becomes $E/(1-2\nu)\ \nabla^2 e = 0$ and finally $\nabla^2 e = 0$, a result that is obtained in the previous section, see eq. (3.3).

3.1.3 Solutions to elasticity problems

Solutions to practical problems in three dimensions are very difficult to achieve for all but the simplest geometries. This is largely due to the large number of partial differential equations in the governing equations of linear elasticity and the fact that solutions to partial differential equations involve arbitrary functions (rather than the

much simpler arbitrary constants that occur in solutions to ordinary differential equations). The choice of such functions generally depends critically on the particular geometry of the problem under consideration. In this section, one single problem will be treated to illustrate the difficulty of the solution procedure.

Example 3.1. Rectangular bar hanging under its own weight

To illustrate the solution problem for a simple practical problem, the stress and displacement distributions in a prismatic bar hanging vertically under its own weight will be evaluated. For simplicity, consider a prismatic bar of length L, with a rectangular cross-section of width b and thickness t, hanging vertically under the action of gravity as shown in fig. 3.2. The cross-sectional dimensions of the bar are assumed to be far smaller than its length, *i.e.*, $b/L \ll 1$ and $t/L \ll 1$.

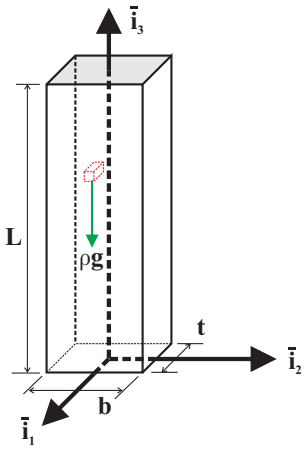

Fig. 3.2. Prismatic bar hanging under its own weight.

While a number of approaches to this problem are possible, perhaps the simplest is to seek a solution for the stress field. This is a natural choice because all the sides of the bar are stress-free, except for the top surface where it is attached to the support. Expressing these stress-free boundary conditions is relatively easy in a stress based formulation. While the six Beltrami-Michell equations, eqs. (3.4), could be used as the starting point of this development, it is easier to adopt a semi-inverse method, in which simplifying assumptions are made prior to solving the governing equations.

Because the cross-sectional dimensions of the bar are small compared to its length, it seems reasonable to assume that, *(1)* all transverse stress components vanish, and *(2)* the axial stress, σ_3, is solely a function of the variable x_3. With these simplifications, the three equilibrium equations reduce to the single equation, $\mathrm{d}\sigma_3/\mathrm{d}x_3 + b_3 = 0$. The applied load per unit volume of the bar is $b_3 = -\rho g$, where ρ is the material mass density and g the gravitational constant; this equation is in-

tegrated to find the axial stress component, σ_3, as $\sigma_3 = \int -b_3 \, \mathrm{d}x_3 = \rho g x_3 + C$, where C is an integration constant.

The stress boundary conditions can be expressed using eq. (1.9), but since all surfaces are perpendicular to one of the coordinate axes, it follows that $\sigma_1 = \tau_{12} = \tau_{13} = 0$ on faces normal to axis $\bar{\imath}_1$, $\sigma_2 = \tau_{21} = \tau_{23} = 0$ on faces normal to $\bar{\imath}_2$, and $\sigma_3 = \tau_{31} = \tau_{32} = 0$ on the lower face. The assumed stress state satisfies all these boundary conditions except for the condition that $\sigma_3 = 0$ on the lower face. Imposing this condition on the stress field yields $C = 0$ and hence,

$$\sigma_3 = \rho g x_3. \tag{3.5}$$

All all other stress components vanish. This solution implies that the stress on the upper surface, at $x_3 = L$, is $\sigma_3 = \rho g L$. The net force on this area is the integral of the stress over the cross-section, which is equal to $\rho g L b t$, the total weight of the bar, as expected from elementary statics.

Now that the stress field throughout the body has been established, the corresponding displacement field must be evaluated. The first step in determining the displacement components is to express the strains in terms of the stresses using the constitutive equations (2.4) and (2.8) to find

$$\epsilon_1 = -\frac{\nu \rho g x_3}{E}, \; \epsilon_2 = -\frac{\nu \rho g x_3}{E}, \; \epsilon_3 = \frac{\rho g x_3}{E}, \; \gamma_{12} = \gamma_{13} = \gamma_{23} = 0. \tag{3.6}$$

The shear strain components vanish, while the direct strain components are linear functions of x_3, hence, all six compatibility equations (1.106) are satisfied.

To determine the displacements, it is necessary to integrate the strain-displacement equations (1.63) and (1.71) which can be stated as follows

$$\frac{\partial u_1}{\partial x_1} = -\frac{\nu \rho g}{E} x_3, \tag{3.7a}$$

$$\frac{\partial u_2}{\partial x_2} = -\frac{\nu \rho g}{E} x_3, \tag{3.7b}$$

$$\frac{\partial u_3}{\partial x_3} = \frac{\rho g}{E} x_3, \tag{3.7c}$$

$$\frac{\partial u_1}{\partial x_2} + \frac{\partial u_2}{\partial x_1} = 0, \tag{3.7d}$$

$$\frac{\partial u_1}{\partial x_3} + \frac{\partial u_3}{\partial x_1} = 0, \tag{3.7e}$$

$$\frac{\partial u_2}{\partial x_3} + \frac{\partial u_3}{\partial x_2} = 0. \tag{3.7f}$$

Integration of these partial differential equations to determine the displacement field turns out to be a bit more challenging than it appears. Integrating eq. (3.7c) yields the third displacement component as

$$u_3 = \frac{\rho g}{2E} x_3^2 + f_1(x_1, x_2), \tag{3.8}$$

where the constant of partial integration is a function, $f_1(x_1, x_2)$, rather than simply a constant, as would be the case for ordinary differential equations. This result can now be substituted into equations (3.7e) and (3.7f) to find $\partial u_1/\partial x_3 = -\partial f_1/\partial x_1$ and $\partial u_2/\partial x_3 = -\partial f_1/\partial x_2$. These equations can be integrated to yield

$$u_1 = -\frac{\partial f_1}{\partial x_1} x_3 + f_2(x_1, x_2), \quad u_2 = -\frac{\partial f_1}{\partial x_2} x_3 + f_3(x_1, x_2), \tag{3.9}$$

where $f_2(x_1, x_2)$ and $f_3(x_1, x_2)$ are arbitrary functions arising from the integration. While eqs. (3.7c), (3.7e) and (3.7f) have been used already, the above displacements can be substituted into eqs. (3.7a) and (3.7b) to find $-(\partial^2 f_1/\partial x_1^2)\, x_3 + (\partial f_2/\partial x_1) = -(\nu\rho g/E)\, x_3$ and $-(\partial^2 f_1/\partial x_2^2)\, x_3 + (\partial f_3/\partial x_2) = -(\nu\rho g/E)\, x_3$, which can be rearranged into a more useful form as

$$\left(\frac{\partial^2 f_1}{\partial x_1^2} - \frac{\nu\rho g}{E}\right) x_3 = \frac{\partial f_2}{\partial x_1}, \quad \left(\frac{\partial^2 f_1}{\partial x_2^2} - \frac{\nu\rho g}{E}\right) x_3 = \frac{\partial f_3}{\partial x_2}. \tag{3.10}$$

These results must be carefully examined: functions $f_1(x_1, x_2)$, $f_2(x_1, x_2)$, and $f_3(x_1, x_2)$ are all three independent of x_3. Because the above equations must hold for any value of x_3, the expressions in parentheses, which depend only on x_1 and x_2, must vanish, as must the righthand sides of the equations, implying that

$$\frac{\partial^2 f_1}{\partial x_1^2} = \frac{\nu\rho g}{E}, \tag{3.11a}$$

$$\frac{\partial^2 f_1}{\partial x_2^2} = \frac{\nu\rho g}{E}, \tag{3.11b}$$

$$\frac{\partial f_2}{\partial x_1} = 0, \tag{3.11c}$$

$$\frac{\partial f_3}{\partial x_2} = 0. \tag{3.11d}$$

These expressions are still insufficient to determine the functions $f_1(x_1, x_2)$, $f_2(x_1, x_2)$ and $f_3(x_1, x_2)$, but eq. (3.7d) has not yet been used. Substituting u_1 and u_2 from eq. (3.9) into eq. (3.7d) yields

$$-2\frac{\partial^2 f_1}{\partial x_1 \partial x_2} x_3 + \frac{\partial f_3}{\partial x_1} + \frac{\partial f_2}{\partial x_2} = 0.$$

The reasoning used earlier applies here again: because the above equation must hold for any value of x_3 and because f_2 and f_3 are functions of x_1 and x_2 only, both the coefficient of x_3 and the independent term must vanish, leading to

$$\frac{\partial^2 f_1}{\partial x_1 \partial x_2} = 0 \tag{3.12a}$$

$$\frac{\partial f_3}{\partial x_1} + \frac{\partial f_2}{\partial x_2} = 0. \tag{3.12b}$$

Equations (3.11) and (3.12) now constitute a set of equations that can be solved for the unknown functions f_1, f_2 and f_3. Equations (3.11c) and (3.11d) can be integrated to yield $f_2 = C_1 a_1(x_2) + C_2$ and $f_3 = C_3 a_2(x_1) + C_4$, where $a_1(x_2)$ and $a_2(x_1)$ are arbitrary functions and C_1, C_2, C_3 and C_4 arbitrary constants. Substituting these into eq. (3.12b) results in

$$C_3 \frac{\mathrm{d}a_2(x_1)}{\mathrm{d}x_1} + C_1 \frac{\mathrm{d}a_1(x_2)}{\mathrm{d}x_2} = 0,$$

where the functional dependence is explicitly shown and the partial derivatives become regular derivatives. Inspection of this result reveals that the only possible solution is $a_1 = x_2$, $a_2 = x_1$ and $C_3 = -C_1$, leading to

$$f_2 = C_1 x_2 + C_2 \quad \text{and} \quad f_3 = -C_1 x_1 + C_4. \tag{3.13}$$

Next, eqs. (3.11a) and (3.11b) can be integrated to yield two different expressions for f_1: $f_1 = (\nu\rho g/2E)\ x_1^2 + f_4(x_2)\ x_1 + C_5$ and $f_1 = (\nu\rho g/2E)\ x_2^2 + f_5(x_1)\ x_2 + C_6$. Equation (3.12a) now implies $(\partial^2 f_1)/(\partial x_1 \partial x_2) = \mathrm{d}f_4/\mathrm{d}x_2 = 0$ and $(\partial^2 f_1)/(\partial x_1 \partial x_2) = \mathrm{d}f_5/\mathrm{d}x_1 = 0$, and hence, $f_4 = C_7$ and $f_5 = C_8$. Finally, it is possible to combine these results into a single expression for f_1

$$f_1 = \frac{\nu\rho g}{2E}(x_1^2 + x_2^2) + C_7 x_1 + C_8 x_2 + C_9, \tag{3.14}$$

where the C_7, C_8 and C_9 are arbitrary constants. The functions expressed in eqs. (3.13) and (3.14) can now be substituted into eqs. (3.8) and (3.9) to yield solutions for the displacement components

$$\begin{aligned} u_1 &= -\frac{\nu\rho g}{E} x_1 x_3 - C_7 x_3 + C_1 x_2 + C_3, \\ u_2 &= -\frac{\nu\rho g}{E} x_2 x_3 - C_8 x_3 - C_1 x_1 + C_4, \\ u_3 &= \frac{\rho g}{2E} x_3^2 + \frac{\nu\rho g}{2E}(x_1^2 + x_2^2) + C_7 x_1 + C_8 x_2 + C_9. \end{aligned} \tag{3.15}$$

At this point, the only remaining task is to determine the integration constants appearing in the displacement field. Two requirements must be met: the bar undergoes no rigid body translation and no rigid body rotation. The simplest way to impose these conditions is to enforce the vanishing of displacements and rotations at the center of the upper surface along which the bar is attached: vanishing of the displacements implies $u_1(0,0,L) = u_2(0,0,L) = u_3(0,0,L) = 0$, whereas vanishing of the rotations leads to $\omega_1(0,0,L) = \omega_2(0,0,L) = \omega_3(0,0,L) = 0$, see eqs. (1.73). Application of these boundary conditions to the displacement field given by eq. (3.15) is left as an exercise; the final expression for the displacement field is

$$u_1 = -\frac{\nu\rho g}{E} x_1 x_3,\ u_2 = -\frac{\nu\rho g}{E} x_2 x_3,\ u_3 = \frac{\rho g}{2E}\left[x_3^2 - L^2 + \nu(x_1^2 + x_2^2)\right]. \tag{3.16}$$

Equations (3.5) and (3.16) describe the state of stress and displacement, respectively, inside the prismatic bar hanging vertically under its own weight. A number of

features of this solution are worth examining in more detail. The stress field consists of a single component, σ_3, which linearly increases from the lower to the upper end of the bar, as expected from basic statics requirements. The displacement solution is a bit more complex but quite revealing. The vertical displacement of the lower surface of the bar, *i.e.*, at $x_3 = 0$, is given by

$$u_3(x_3 = 0) = -\frac{\rho g}{2E}\left[L^2 - \nu(x_1^2 + x_2^2)\right].$$

Figure 3.3 shows this distribution of non-dimensional displacement, $u_3/(\rho g/2EL^2)$, over the cross-section of the bar. The vertical displacement at the centerline, *i.e.*, at $x_1 = x_2 = 0$, is that which would be obtained from a one dimensional analysis ignoring the finite dimension of the cross-section. The vertical displacement away from the centerline is reduced by a factor proportional to Poisson's ratio and the square of the distance from the centerline, resulting in a spherical shape for the deflected surface; the central portion of the bar deflects more than the outer regions. The vertical displacement of the upper surface vanishes only at the centerline, as required by the imposed boundary conditions, but is otherwise parabolic. These results are consistent with the stress-free boundary conditions assumed at the lower surface, but had the upper surface been assumed to remain planar, a completely different solution would have resulted. This behavior is perhaps easier to visualize if one imagines the bar to be made of a very soft material like gelatin; in this case, the parabolic displacement of the bar's cross-section becomes more intuitive.

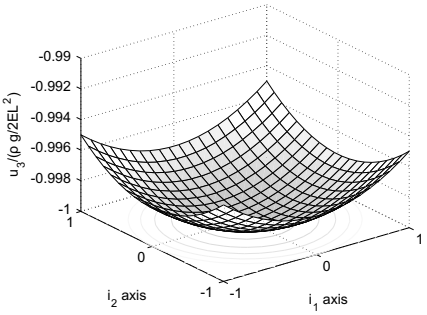

Fig. 3.3. Vertical displacement component, u_3, of lower surface of the prismatic bar.

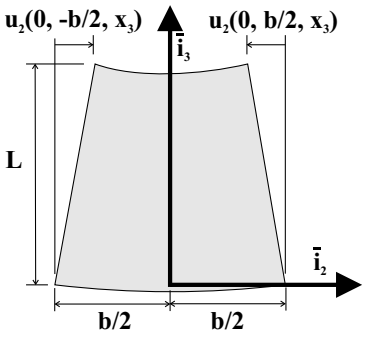

Fig. 3.4. Lateral displacement component, u_2, of the left and right sides of prismatic bar.

The displacements of the sides of the bar reveal additional details of the deformation behavior. Figure 3.4 shows a greatly exaggerated plot of the shape of a section of the bar taken through the centerline and perpendicular to axis $\bar{\imath}_1$. As indicated by eq. (3.16), the sides of the bar taper inwards for increasing values of x_3 so that the transverse dimensions of the upper cross-section are smaller than those of the lower. This behavior is due to Poisson's effect, and the presence of Poisson's ratio, ν, in the equations for u_1 and u_2 clearly indicates the origin of this phenomenon.

3.2 Plane strain problems

The assumption of plane strain state introduced in section 1.6 reduces three-dimensional problems to two-dimensional problems and results in considerable simplification of the governing equations. In plane strain problems, the displacements, body forces and changes in properties are assumed to vanish along a preferential direction; it is always possible to select axis $\bar{\imath}_3$ to coincide with that preferential direction. Problems meeting these conditions are not necessarily two-dimensional in appearance, such as a thin sheet or a flat plate, but instead, experience no deformation in one direction. For example, the cross-section of a buried pipe or a cross-section of a long dam could be modeled as plane strain problems under the assumption that there is no displacement in the axial direction.

For plane strain states, the strain-displacement equations, eqs. (1.63) and (1.71), reduce to

$$\epsilon_1 = \frac{\partial u_1}{\partial x_1}, \quad \epsilon_2 = \frac{\partial u_2}{\partial x_2}, \quad \gamma_{12} = \frac{\partial u_1}{\partial x_2} + \frac{\partial u_2}{\partial x_1}, \tag{3.17}$$

while the axial and transverse shear strain components vanish, $\epsilon_3 = \gamma_{13} = \gamma_{23} = 0$. Similarly, the equilibrium equations, eqs. (1.4), reduce to

$$\frac{\partial \sigma_1}{\partial x_1} + \frac{\partial \tau_{21}}{\partial x_2} + b_1 = 0, \quad \frac{\partial \tau_{12}}{\partial x_1} + \frac{\partial \sigma_2}{\partial x_2} + b_2 = 0. \tag{3.18}$$

The transverse shear stress components vanish, $\tau_{13} = \tau_{23} = 0$, while the axial stress does not due to Poisson's effect, $\sigma_3 = \nu(\sigma_1 + \sigma_2)$. If the material is assumed to obey Hooke's law, the vanishing of the axial and transverse shear strain components results in the following reduced constitutive laws

$$\epsilon_1 = \frac{1+\nu}{E}\left[(1-\nu)\sigma_1 - \nu\sigma_2\right], \; \epsilon_2 = \frac{1+\nu}{E}\left[(1-\nu)\sigma_2 - \nu\sigma_1\right], \; \gamma_{12} = \frac{\tau_{12}}{G}. \tag{3.19}$$

Under plane strain assumptions, Navier's equations, eqs. (3.1), reduce to two equations only,

$$\frac{E}{2(1+\nu)(1-2\nu)}\frac{\partial e}{\partial x_1} + G\,\nabla^2 u_1 + b_1 = 0, \tag{3.20a}$$

$$\frac{E}{2(1+\nu)(1-2\nu)}\frac{\partial e}{\partial x_2} + G\,\nabla^2 u_2 + b_2 = 0, \tag{3.20b}$$

where the volumetric strain, see eq. (1.75), reduces to $e = \epsilon_1 + \epsilon_2$. The differential operator ∇^2 is now the *two-dimensional Laplacian*

$$\nabla^2 = \frac{\partial^2}{\partial x_1^2} + \frac{\partial^2}{\partial x_2^2}. \tag{3.21}$$

Taking derivatives with respect to x_1 and x_2 of eqs. (3.20a) and (3.20b), respectively, and summing up the resulting equations leads to

$$\frac{2(1-\nu)G}{1-2\nu}\nabla^2 e = -\left(\frac{\partial b_1}{\partial x_1} + \frac{\partial b_2}{\partial x_2}\right). \tag{3.22}$$

The constitutive law for the volumetric strain, given by eq. (2.18), reduces to $e = (1-2\nu)(1+\nu)(\sigma_1+\sigma_2)/E$ for plane strain state. It then follows that

$$\nabla^2(\sigma_1+\sigma_2) = -\frac{1}{1-\nu}\left(\frac{\partial b_1}{\partial x_1} + \frac{\partial b_2}{\partial x_2}\right). \tag{3.23}$$

Unfortunately, this equation alone is insufficient to determine the three stress components, σ_1, σ_2 and τ_{12}. To overcome this problem, a novel approach, first proposed by Airy, is introduced. It is assumed that the body forces, b_1 and b_2, are *conservative forces*, *i.e.*, they can be derived from a potential: $b_1 = -\partial V/\partial x_1$ and $b_2 = -\partial V/\partial x_2$, where $V(x_1, x_2)$ is the *potential of the body forces*. Next, the stress field is written in terms of *Airy's stress function*, $\phi(x_1, x_2)$, as

$$\sigma_1 = \frac{\partial^2\phi}{\partial x_2^2} + V, \quad \sigma_2 \quad = \frac{\partial^2\phi}{\partial x_1^2} + V, \quad \tau_{12} = -\frac{\partial^2\phi}{\partial x_1 \partial x_2}. \tag{3.24}$$

The stress field written in terms of Airy's stress function *automatically satisfies the equilibrium equations of the problem*, as can be verified by introducing eqs. (3.24) into eqs. (3.18). This is the very reason why Airy's stress function is introduced in the first place: instead of working with three stress components, σ_1, σ_2 and τ_{12}, a single unknown, the stress function, ϕ, remains. Furthermore, the stress field derived from Airy's stress function through eqs. (3.24) automatically satisfies equilibrium conditions.

Introducing the stress components expressed in terms of Airy's stress function into equilibrium equation (3.23) yields a single equation for the stress function

$$\frac{\partial^4\phi}{\partial x_1^4} + 2\frac{\partial^4\phi}{\partial x_1^2 \partial x_2^2} + \frac{\partial^4\phi}{\partial x_2^4} = \nabla^4\phi = -\frac{1-2\nu}{1-\nu}\nabla^2 V. \tag{3.25}$$

This is a nonhomogeneous, two-dimensional *bi-harmonic partial differential equation*. When the body forces vanish or are harmonic function, *i.e.*, when $\nabla^2 V = 0$, the governing equation becomes the homogeneous bi-harmonic equation. The bi-harmonic equation has been extensively studied and a number of solution procedures are available.

3.3 Plane stress problems

The assumption of plane stress state introduced in section 1.3 reduces three-dimensional problems to two-dimensional problems and results in considerable simplification of the governing equations. In plane stress problems, the stress components and body forces are assumed to vanish along a preferential direction. It is always possible to select axis $\bar{\imath}_3$ to coincide with that preferential direction; hence $\sigma_3 = \tau_{13} = \tau_{23} = 0$ and $b_3 = 0$. Next, it is assumed that the response of the solid

does not vary along axis $\bar{\imath}_3$, leading to further simplification of the governing equations. This latter assumption is realistic for bodies in the form of thin sheets loaded by forces acting in the plane of the sheet.

For plane stress states, the equilibrium equations are identical to those for plane strain states, eqs. (3.18). If the material is assumed to obey Hooke's law, the vanishing of the axial and shear stress components leads to the following reduced constitutive laws

$$\epsilon_1 = \frac{1}{E}(\sigma_1 - \nu\sigma_2), \quad \epsilon_2 = \frac{1}{E}(\sigma_2 - \nu\sigma_1), \quad \gamma_{12} = \frac{1}{G}\tau_{12}. \tag{3.26}$$

The inverse relationships are

$$\sigma_1 = \frac{E}{1-\nu^2}(\epsilon_1 + \nu\epsilon_2), \quad \sigma_2 = \frac{E}{1-\nu^2}(\epsilon_2 + \nu\epsilon_1), \quad \tau_{12} = G\,\gamma_{12}, \tag{3.27}$$

Finally, the strain along axis $\bar{\imath}_3$ is $\epsilon_3 = -\nu(\sigma_1 + \sigma_2)/E$. Although Hooke's law is used for both plane strain and plane stress problems, the reduced constitutive law differ for the two cases, see eqs (3.19) and (3.26), respectively.

It is convenient here again to use Airy's stress function to satisfy equilibrium conditions and substitute the stress components expressed in terms of the stress function, eq. (3.24), into the constitutive equations to obtain the following expressions for the strain components

$$\epsilon_1 = \frac{1}{E}\left[\frac{\partial^2\phi}{\partial x_2^2} - \nu\frac{\partial^2\phi}{\partial x_1^2} + (1-\nu)V\right], \; \epsilon_2 = \frac{1}{E}\left[\frac{\partial^2\phi}{\partial x_1^2} - \nu\frac{\partial^2\phi}{\partial x_2^2} + (1-\nu)V\right]$$
$$\epsilon_3 = -\frac{\nu}{E}\left[\frac{\partial^2\phi}{\partial x_2^2} + \frac{\partial^2\phi}{\partial x_1^2} + 2V\right], \quad \gamma_{12} = -\frac{1}{G}\frac{\partial^2\phi}{\partial x_1 \partial x_2}.$$

Of course, the transverse shear strain components vanish, $\gamma_{13} = \gamma_{23} = 0$.

These strain components can be substituted into the strain compatibility equations (1.106c), (1.106b), (1.106a) and (1.106f) to obtain

$$\nabla^4\phi = -(1-\nu)\nabla^2 V, \tag{3.28a}$$
$$\frac{\partial^2\epsilon_3}{\partial x_1^2} = \frac{\partial^4\phi}{\partial x_1^4} + \frac{\partial^4\phi}{\partial x_1^2\partial x_2^2} + 2\frac{\partial^2 V}{\partial x_1^2} = 0, \tag{3.28b}$$
$$\frac{\partial^2\epsilon_3}{\partial x_2^2} = \frac{\partial^4\phi}{\partial x_2^4} + \frac{\partial^4\phi}{\partial x_1^2\partial x_2^2} + 2\frac{\partial^2 V}{\partial x_2^2} = 0, \tag{3.28c}$$
$$\frac{\partial^2\epsilon_3}{\partial x_1\partial x_2} = \frac{\partial^4\phi}{\partial x_1^3\partial x_2} + \frac{\partial^4\phi}{\partial x_1\partial x_2^3} + 2\frac{\partial^2 V}{\partial x_1\partial x_2} = 0, \tag{3.28d}$$

respectively, while the last two compatibility equations, eqs. (1.106d) and (1.106e), are automatically satisfied. This appears to be a complicated situation with four equations to define the stress function. It can be shown, however, that failure to satisfy the last three equations, eqs. (3.28b) to (3.28d), does not lead to large errors. Hence, a single equation for Airy's stress function remains

$$\nabla^4\phi = -(1-\nu)\nabla^2 V. \tag{3.29}$$

When the body forces vanish or are harmonic function, *i.e.*, when $\nabla^2 V = 0$, the governing equation becomes the homogeneous bi-harmonic equation, as is the case for the plane strain state.

In conclusion, both plane strain and plane stress states lead to nonhomogeneous bi-harmonic equations, eqs. (3.25) and (3.29), respectively. The two equations present only slight differences in their nonhomogeneous parts. For plane strain and plane stress problems, boundary conditions will differ considerably and the constitutive relationships are also different; hence, identical solutions of the two problems should not be expected. Nonetheless, the wealth of knowledge about how to solve bi-harmonic equations is useful for both types of problems.

3.4 Plane strain and plane stress in polar coordinates

A number of practical plane strain or plane stress problems present circular boundaries or cylindrical symmetry. Examples include such problems as thick-walled tubes subjected to torsion or internal pressure, thin sheets with circular holes, curved beams and many others.

To formulate these types of problems, the governing equations of elasticity must be recast in a polar (or cylindrical) coordinate system. While this can be accomplished by re-examination of differential volume and area elements defined in the cylindrical coordinate system, the equations can also be obtained from those derived in Cartesian coordinates through appropriate transformations. To this end, consider the coordinate system $(\bar{\imath}_1, \bar{\imath}_2)$ that forms the basis of a Cartesian system and the unit vectors of the polar system, $(\bar{\imath}_r, \bar{\imath}_\theta)$, as depicted fig. 3.5.

Polar coordinates are expressed in terms of their Cartesian counterparts through the following well-known relationships

$$r = \sqrt{x_1^2 + x_2^2}, \quad \theta = \arctan\frac{x_2}{x_1}, \tag{3.30}$$

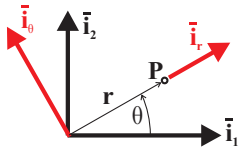

Fig. 3.5. Coordinate rotation from Cartesian into Polar.

where r is the radial coordinate and θ is the angular coordinate, while the inverse transformation is readily obtained as

$$x_1 = r\ \cos\theta, \quad x_2 = r\ \sin\theta. \tag{3.31}$$

Transformations of the displacement components expressed in the two coordinates systems are particular cases of the transformations expressed by eqs. (A.43), recast as

$$\begin{Bmatrix} u_r \\ u_\theta \end{Bmatrix} = \begin{bmatrix} \cos\theta & \sin\theta \\ -\sin\theta & \cos\theta \end{bmatrix} \begin{Bmatrix} u_1 \\ u_2 \end{Bmatrix}, \quad \begin{Bmatrix} u_1 \\ u_2 \end{Bmatrix} = \begin{bmatrix} \cos\theta & -\sin\theta \\ \sin\theta & \cos\theta \end{bmatrix} \begin{Bmatrix} u_r \\ u_\theta \end{Bmatrix}. \tag{3.32}$$

It will also be necessary to express the transformations of partial derivatives with respect to both coordinates system. The chain rule for derivatives implies that $\partial/\partial x_1 = (\partial/\partial r)(\partial r/\partial x_1) + (\partial/\partial\theta)(\partial\theta/\partial x_1)$, with a similar expression for the partial derivative with respect to x_2. It then follows that

$$\begin{Bmatrix} \dfrac{\partial}{\partial x_1} \\ \dfrac{\partial}{\partial x_2} \end{Bmatrix} = \begin{bmatrix} \cos\theta & -\sin\theta \\ \sin\theta & \cos\theta \end{bmatrix} \begin{Bmatrix} \dfrac{\partial}{\partial r} \\ \dfrac{1}{r}\dfrac{\partial}{\partial\theta} \end{Bmatrix}. \tag{3.33}$$

The derivatives of polar coordinates with respect to their Cartesian counterparts are easily developed from eq. (3.30) to find

$$\frac{\partial r}{\partial x_1} = \frac{x_1}{r} = \cos\theta,\ \frac{\partial r}{\partial x_2} = \frac{x_2}{r} = \sin\theta,\ \frac{\partial\theta}{\partial x_1} = -\frac{\sin\theta}{r},\ \frac{\partial\theta}{\partial x_2} = \frac{\cos\theta}{r}. \tag{3.34}$$

Next, the strain components expressed in the two coordinate systems will be related to each other using the general two-dimensional strain rotation expressions given by eqs. (1.91). The radial strain component, ϵ_r, becomes

$$\epsilon_r = \epsilon_1\ \cos^2\theta + \epsilon_2\ \sin^2\theta + \gamma_{12}\ \sin\theta\cos\theta, \tag{3.35}$$

where the Cartesian strain components, ϵ_1, ϵ_2, and γ_{12}, are computed by means of the strain-displacement equations, eqs. (1.63) and (1.71), to find

$$\begin{aligned}
\epsilon_1 =& \frac{\partial u_1}{\partial x_1} = \left(\cos\theta\frac{\partial}{\partial r} - \frac{\sin\theta}{r}\frac{\partial}{\partial\theta}\right)(u_r\cos\theta - u_\theta\sin\theta),\\
\epsilon_2 =& \frac{\partial u_2}{\partial x_2} = \left(\sin\theta\frac{\partial}{\partial r} + \frac{\cos\theta}{r}\frac{\partial}{\partial\theta}\right)(u_r\sin\theta + u_\theta\cos\theta),\\
\gamma_{12} =& \frac{\partial u_1}{\partial x_2} + \frac{\partial u_2}{\partial x_1} = \left(\sin\theta\frac{\partial}{\partial r} + \frac{\cos\theta}{r}\frac{\partial}{\partial\theta}\right)(u_r\cos\theta - u_\theta\sin\theta)\\
&+ \left(\cos\theta\frac{\partial}{\partial r} - \frac{\sin\theta}{r}\frac{\partial}{\partial\theta}\right)(u_r\sin\theta + u_\theta\cos\theta).
\end{aligned}$$

Note that the partial derivatives and displacement components are evaluated with the help of eqs. (3.33) and (3.32), respectively. Finally, these strain components are substituted into eq. (3.35) to find, after considerable algebraic manipulation,

$$\epsilon_r = (\cos^4\theta + 2\sin^2\theta\cos^2\theta + \sin^4\theta)\frac{\partial u_r}{\partial r} = \frac{\partial u_r}{\partial r}. \tag{3.36}$$

A similar procedure can be followed to derive the three components of strain in the polar coordinate system as

$$\epsilon_r = \frac{\partial u_r}{\partial r}, \tag{3.37a}$$

$$\epsilon_\theta = \frac{1}{r}\frac{\partial u_\theta}{\partial\theta} + \frac{u_r}{r}, \tag{3.37b}$$

$$\gamma_{r\theta} = \frac{\partial u_\theta}{\partial r} + \frac{1}{r}\frac{\partial u_r}{\partial\theta} - \frac{u_\theta}{r}. \tag{3.37c}$$

A similar development can be carried out to express stress components in polar coordinates in terms of Airy's stress function. The two-dimensional stress component transformation equations (1.47) are used to express the radial stress component, σ_r, in terms of its Cartesian counterparts to find

$$\begin{aligned}\sigma_r &= \sigma_1 \cos^2\theta + \sigma_2 \sin^2\theta + 2\tau_{12}\sin\theta\cos\theta \\ &= \frac{\partial^2\phi}{\partial x_2^2}\cos^2\theta + \frac{\partial^2\phi}{\partial x_1^2}\sin^2\theta - 2\frac{\partial^2\phi}{\partial x_1 \partial x_2}\sin\theta\cos\theta,\end{aligned}$$

where the Cartesian stress components are expressed in terms of Airy's stress function using eq. (3.24) and body force terms are neglected. The final step is to use eq. (3.33) to express the derivatives with respect to Cartesian coordinates in terms of derivatives with respect to polar coordinates. Tedious algebra then yields

$$\sigma_r = \frac{1}{r}\frac{\partial\phi}{\partial r} + \frac{1}{r^2}\frac{\partial^2\phi}{\partial\theta^2}.$$

The same procedure can be used to obtain expressions for the remaining stress components in polar coordinates, leading to

$$\sigma_r = \frac{1}{r}\frac{\partial\phi}{\partial r} + \frac{1}{r^2}\frac{\partial^2\phi}{\partial\theta^2}, \tag{3.38a}$$

$$\sigma_\theta = \frac{\partial^2\phi}{\partial r^2}, \tag{3.38b}$$

$$\tau_{r\theta} = \frac{1}{r^2}\frac{\partial\phi}{\partial\theta} - \frac{1}{r}\frac{\partial^2\phi}{\partial r\partial\theta}. \tag{3.38c}$$

To obtain a complete set of governing equations, it is also necessary to express the two equilibrium equations in polar coordinates. Figure 3.6 shows a differential element of area in polar coordinates with normal and shear stresses acting on each of its four faces. Since the stress state is assumed to vary smoothly, stress components on opposite faces of the differential element are expanded in Taylor series, using the first term of the series only.

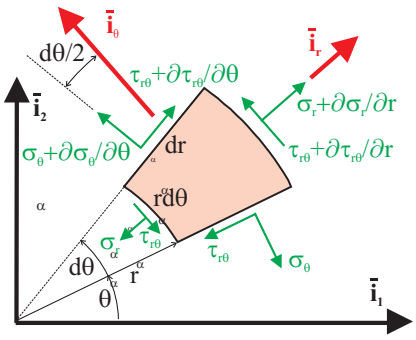

Fig. 3.6. Stresses acting on a differential area defined in polar coordinates.

The first equilibrium equation is obtained by projecting all forces along axis $\bar{i}_r$. Forces are obtained by multiplying the the stress components by the area on which they act, and a unit thickness of the volume element is assumed. Note that in view of the shape of the element, the circumferential stress component, σ_θ, contributes to the axial equilibrium equation because this components acts in a direction that forms an angle $\mathrm{d}\theta/2$ with axis $\bar{i}_\theta$.

The second equilibrium equation is obtained by projecting forces along axis $\bar{\imath}_\theta$. It is left as an exercise to show that the resulting equilibrium equations are

$$\frac{\partial \sigma_r}{\partial r} + \frac{1}{r}\frac{\partial \tau_{r\theta}}{\partial \theta} + \frac{\sigma_r - \sigma_\theta}{r} = 0, \tag{3.39a}$$

$$\frac{1}{r}\frac{\partial \sigma_\theta}{\partial \theta} + \frac{\partial \tau_{r\theta}}{\partial r} + 2\frac{\tau_{r\theta}}{r} = 0. \tag{3.39b}$$

Finally, since the bi-harmonic equation governs both plane strain and plane stress problems, see eqs. (3.25) and (3.29), respectively, it is necessary to develop an expression for the Laplacian, ∇^2, in polar coordinates. This task is achieved by using eq. (3.33), which relates the derivatives with respect to Cartesian coordinates to derivatives with respect to polar coordinates, to find

$$\begin{aligned}\nabla^2 &= \frac{\partial^2}{\partial x_1^2} + \frac{\partial^2}{\partial x_2^2} = \left(\cos\theta\frac{\partial}{\partial r} - \frac{\sin\theta}{r}\frac{\partial}{\partial \theta}\right)^2 + \left(\sin\theta\frac{\partial}{\partial r} + \frac{\cos\theta}{r}\frac{\partial}{\partial \theta}\right)^2 \\ &= \frac{\partial^2}{\partial r^2} + \frac{1}{r}\frac{\partial}{\partial r} + \frac{1}{r^2}\frac{\partial}{\partial \theta^2}.\end{aligned} \tag{3.40}$$

The bi-harmonic operator then becomes

$$\nabla^4\phi = \left(\frac{\partial^2}{\partial r^2} + \frac{1}{r}\frac{\partial}{\partial r} + \frac{1}{r^2}\frac{\partial^2}{\partial \theta^2}\right)\left(\frac{\partial^2\phi}{\partial r^2} + \frac{1}{r}\frac{\partial\phi}{\partial r} + \frac{1}{r^2}\frac{\partial^2\phi}{\partial \theta^2}\right). \tag{3.41}$$

In the next section, several example problems will be solved to illustrate the use of polar coordinates for problems with cylindrical geometry.

3.5 Problem featuring cylindrical symmetry

Problems featuring cylindrical symmetry, that is, problems for which it is possible to assume that $\partial/\partial\theta = 0$, represent an important class of problems for which solutions are easily obtained because the process developed in the previous sections leads to ordinary, rather than partial differential equations. Such problems are also called *axisymmetric problems,* and the relationship between polar stress components and Airy's stress function, see eq. (3.38), reduces to

$$\sigma_r = \frac{1}{r}\frac{\partial\phi}{\partial r}, \quad \sigma_\theta = \frac{\partial^2\phi}{\partial r^2}, \quad \text{and} \quad \tau_{r\theta} = 0. \tag{3.42}$$

In the absence of body forces, the governing equation for both plane strain and plane stress problems becomes the bi-harmonic equation, see eqs. (3.25) and (3.29), respectively. In view of eq. (3.41), the governing equation becomes

$$\nabla^4\phi = \frac{\mathrm{d}^4\phi}{\mathrm{d}r^4} + \frac{2}{r}\frac{\mathrm{d}^3\phi}{\mathrm{d}r^3} - \frac{1}{r^2}\frac{\mathrm{d}^2\phi}{\mathrm{d}r^2} + \frac{1}{r^3}\frac{\mathrm{d}\phi}{\mathrm{d}r} = 0. \tag{3.43}$$

This is now an ordinary differential equation called the *Euler-Cauchy differential equation*. It can be transformed into an ordinary differential equation with constant coefficients through the following change of variables: $r = e^{\xi}$. Using the chain rule for derivatives, $\mathrm{d}\phi/\mathrm{d}r = (\mathrm{d}\phi/\mathrm{d}\xi)\ (\mathrm{d}\xi/\mathrm{d}r) = e^{-\xi}\ \mathrm{d}\phi/\mathrm{d}\xi$. Equation (3.43) then becomes

$$\frac{\mathrm{d}^4\phi}{\mathrm{d}\xi^4} - 4\frac{\mathrm{d}^3\phi}{\mathrm{d}\xi^3} + 4\frac{\mathrm{d}^2\phi}{\mathrm{d}\xi^2} = 0. \tag{3.44}$$

The solution to this equation is in the form $\phi = e^{z\xi}$, where z is a constant. This leads to the characteristic equation, $z^4 - 4z^3 + 4z^2 = z^2(z-2)^2 = 0$, with solutions $z = 0, 0, 2, 2$. In view of the repeated roots, the solution can then be written as $\phi(\xi) = C_1 + C_2\xi + C_3e^{2\xi} + C_4\xi e^{2\xi}$ in terms of ξ, and finally, in terms of r as

$$\phi(r) = C_1 + C_2 \ln r + C_3r^2 + C_4r^2 \ln r,$$

where C_1, C_2, C_3, and C_4 are integration constants. In view of eq. (3.42), the stress components now become

$$\sigma_r = \frac{1}{r}\frac{\mathrm{d}\phi}{\mathrm{d}r} = \frac{C_2}{r^2} + 2C_3 + C_4(1 + 2\ln r), \quad \sigma_\theta = \frac{\mathrm{d}^2\phi}{\mathrm{d}r^2} = -\frac{C_2}{r^2} + 2C_3 + C_4(3 + 2\ln r). \tag{3.45}$$

Of course, the shear stress still vanishes, *i.e.*, $\tau_{r\theta} = 0$.

The determination of the integration constants and of the displacement field depends on the nature of the problem and the boundary conditions. The examples below illustrate the solution process.

Example 3.2. Thick-walled tube in plane strain state

Figure 3.7 shows a thick-walled cylinder of inner and outer radii, R_i and R_e, respectively, and subjected to internal and external pressures, p_i and p_e, respectively. Determine the stress and displacement distributions through the thickness of the tube.

The problem clearly presents cylindrical symmetry and hence, eq. (3.45) defines the stress state in the tube. In this example, the tube is assumed to be in a state of plane strain, *i.e.*, the axial strain component vanishes.

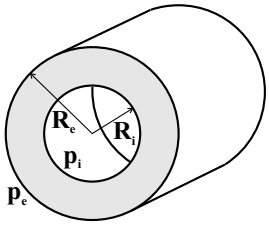

Fig. 3.7. Thick-walled tube subjected to internal and external pressures.

The applied pressures translate into boundary conditions at the inner and outer surfaces of the tube, $\sigma_r(r = R_e) = -p_e$ and $\sigma_r(r = R_i) = -p_i$. No boundary

condition exists for the circumferential stress component, σ_θ, since this stress does not act on any of the boundaries of the system. Using eqs. (3.45), these boundary conditions become

$$-p_e = \frac{C_2}{R_e^2} + 2C_3 + C_4(1 + 2\ln R_e),\ -p_i = \frac{C_2}{R_i^2} + 2C_3 + C_4(1 + 2\ln R_i). \quad (3.46)$$

The solution process now seems to have reached an impasse: three unknown coefficients, C_2, C_3 and C_4, must be evaluated to determine the stress components, but only two boundary conditions, eqs. (3.46), are available. To obtain the missing condition, the other fields of the problem, the strain and displacement fields, must be evaluated. First, the strain components are expressed in terms of their stress counterparts with the help of the constitutive laws, eqs. (3.19), to find

$$\begin{aligned}
\epsilon_r &= \frac{1-\nu^2}{E}\sigma_r - \frac{\nu(1+\nu)}{E}\sigma_\theta = C_a\sigma_r - C_b\sigma_\theta \\
&= C_a\left[\frac{C_2}{r^2} + 2C_3 + C_4(1 + 2\ln r)\right] - C_b\left[-\frac{C_2}{r^2} + 2C_3 + C_4(3 + 2\ln r)\right], \\
\epsilon_\theta &= \frac{1-\nu^2}{E}\sigma_\theta - \frac{\nu(1+\nu)}{E}\sigma_r = C_a\sigma_\theta - C_b\sigma_r \\
&= C_a\left[-\frac{C_2}{r^2} + 2C_3 + C_4(3 + 2\ln r)\right] - C_b\left[\frac{C_2}{r^2} + 2C_3 + C_4(1 + 2\ln r)\right],
\end{aligned}$$

where $C_a = (1-\nu^2)/E$ and $C_b = \nu(1+\nu)/E$.

For problems presenting cylindrical symmetry, the strain-displacement equations, eqs. (3.37), reduce to $\epsilon_r = \mathrm{d}u_r/\mathrm{d}r$ and $\epsilon_\theta = u_r/r$. Eliminating the radial displacement components from these two equations yields the strain compatibility condition: $\epsilon_r - \epsilon_\theta = r\,\mathrm{d}\epsilon_\theta/\mathrm{d}r$. Introducing the strain components computed above yields the following condition: $4C_aC_4 = 0$, and finally, $C_4 = 0$.

Equations (3.46) now involve only two unknown coefficients, which are easily found as $C_2 = -R_i^2R_e^2(p_i - p_e)/(R_e^2 - R_i^2)$ and $C_3 = (R_i^2p_i - R_e^2p_e)/2(R_e^2 - R_i^2)$, leading to the following expressions for the two stress components

$$\begin{aligned}
\sigma_r(r) &= \frac{R_i^2p_i - R_e^2p_e}{R_e^2 - R_i^2} - \frac{1}{r^2}\frac{(p_i - p_e)R_i^2R_e^2}{R_e^2 - R_i^2}, \\
\sigma_\theta(r) &= \frac{R_i^2p_i - R_e^2p_e}{R_e^2 - R_i^2} + \frac{1}{r^2}\frac{(p_i - p_e)R_i^2R_e^2}{R_e^2 - R_i^2}.
\end{aligned} \quad (3.47)$$

In view of the assumption of plane strain state, $\epsilon_3 = 0$ and $u_3 = 0$ and $\sigma_3 = \nu(\sigma_r + \sigma_\theta) = 2\nu(p_iR_i^2 - p_eR_e^2)/(R_e^2 - R_i^2)$: the axial stress component is constant through the thickness of the pipe. Since the shear stress components vanish, stress components σ_r, σ_θ, and σ_3 are, in fact, the principal stresses. Von Mises' equivalent stress is then readily obtained from eq. (2.32) as $2\sigma_{\mathrm{eq}}^2 = (\sigma_r - \sigma_\theta)^2 + (\sigma_\theta - \sigma_3)^2 + (\sigma_3 - \sigma_r)^2$.

Figures 3.8 (a), (b) and (c) show the non-dimensional radial stress, σ_r/p_i, hoop stress, σ_θ/p_i, and Von Mises' equivalent stress, σ_e/p_i, respectively, when the cylinder is subjected to an internal pressure, p_i, *i.e.*, when $p_e = 0$. Results are presented

for three different ratios of the outer to inner radii ($\bar{R} = R_e/R_i$ = 1.5, 2.0 and 3.0). The radial stress is compressive through the thickness of the cylinder and vanishes at the outer radial location, whereas the hoop stress is tensile. The maximum stress component is the hoop stress at $r = R_i$. A similar behavior is observed for the various values of $\bar{R}$. Clearly, von Mises' equivalent stress peaks at the inner radial location, *i.e.*, yield will initiate at the inside surface of the thick cylinder.

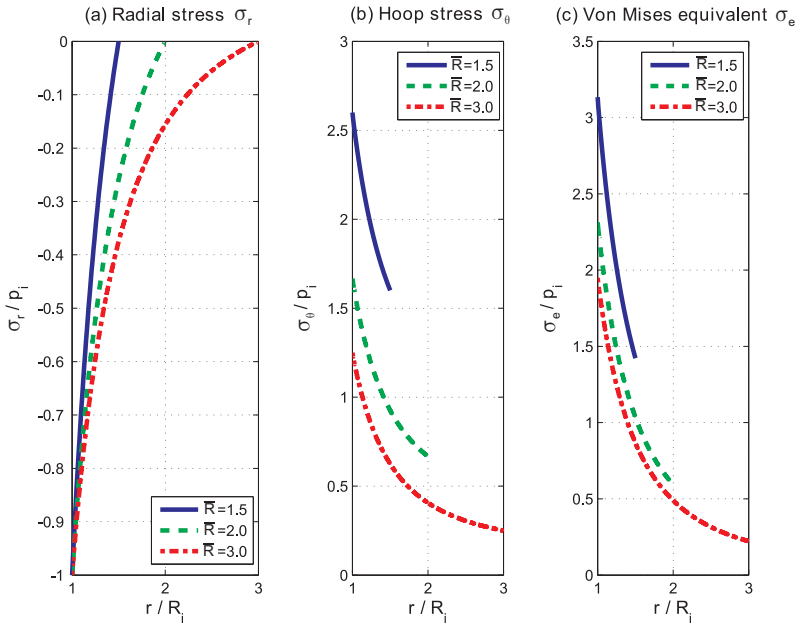

Fig. 3.8. Plots of the non-dimensional radial stress, σ_r/p_i, hoop stress, σ_θ/p_i, and Von Mises' equivalent stress, σ_e/p_i, for three different thickness ratios $\bar{R} = 1.5, 2.0, 3.0$.

The radial and hoop strain components are readily obtained from the constitutive laws, and finally, the radial displacement field is obtained as $u_r = r\epsilon_\theta$, leading to

$$u_r(r) = \frac{(1+\nu)(1-2\nu)}{E}\frac{R_i^2 p_i - R_e^2 p_e}{R_e^2 - R_i^2} r + \frac{1+\nu}{E}\frac{(p_i - p_e)R_i^2 R_e^2}{R_e^2 - R_i^2}\frac{1}{r}. \qquad (3.48)$$

Figures 3.9 (a), (b) and (c) show the non-dimensional radial strain, $E\epsilon_r/p_i$, hoop strain, $E\epsilon_\theta/p_i$, and radial displacement, $Eu_r/(R_i p_i)$, respectively, when the cylinder is subjected to an internal pressure, p_i, *i.e.*, when $p_e = 0$. Results are presented for three different ratios of the outer to inner radii ($\bar{R} = R_e/R_i$ = 1.5, 2.0 and 3.0).

Example 3.3. Thick-walled tube in plane stress state

Figure 3.7 shows a thick-walled cylinder of inner and outer radii, R_i and R_e, respectively, and subjected to internal and external pressures, p_i and p_e, respectively. In

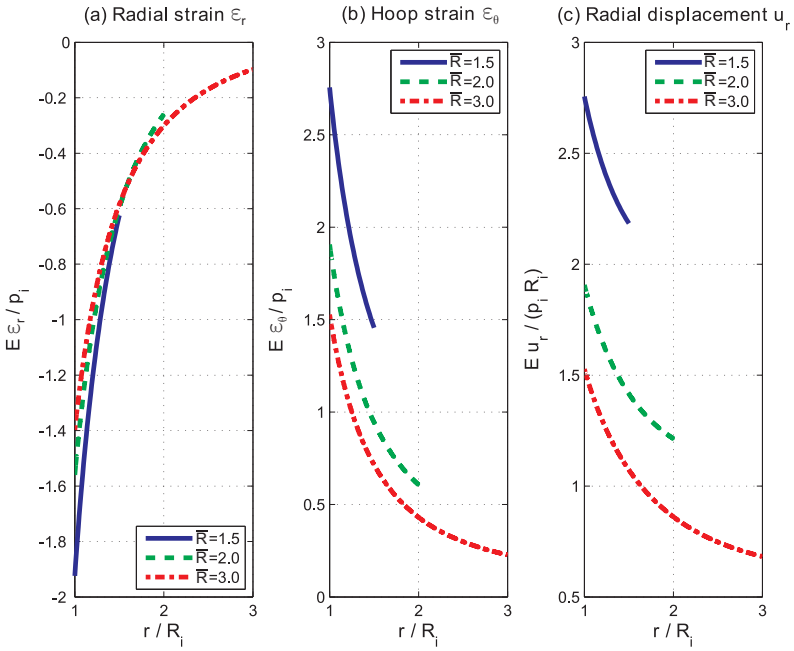

Fig. 3.9. Plots of the non-dimensional radial strain, $E\epsilon_r/p_i$, hoop strain $E\epsilon_\theta/p_i$, and radial displacement, $Eu_r/(R_i p_i)$, for three different thickness ratios $\bar{R} = 1.5, 2.0, 3.0$.

this example, the cylinder is assumed to be in a *state of plane stress*, in contrast with the plane strain assumption of example 3.2. Determine the stress and displacement distributions through the thickness of the tube.

The approach followed in the previous example could be used again here but with the constitutive laws associated with the plane stress state rather than those corresponding to the plane strain state. Instead of using Airy's stress function to satisfy the stress equilibrium and the compatibility equations, a displacement approach is used in this example.

It is assumed here that the cylinder is closed at both ends; hence, it is subjected to an axial load, $\pi R_i^2 p_i - \pi R_e^2 p_e$, which is assumed to be uniformly distributed over the cross-section of the tube, $\pi R_e^2 - \pi R_i^2$, leading to an axial stress

$$\sigma_3 = \frac{R_i^2 p_i - R_e^2 p_e}{R_e^2 - R_i^2}. \tag{3.49}$$

The constitutive laws for the material are given by Hooke's law, eqs. (2.4a) and (2.4b), as $E\epsilon_r = \sigma_r - \nu(\sigma_\theta + \sigma_3)$ and $E\epsilon_\theta = \sigma_\theta - \nu(\sigma_r + \sigma_3)$, respectively. Once recast in a matrix form, these relationships are readily inverted to find

$$\begin{Bmatrix} \sigma_r \\ \sigma_\theta \end{Bmatrix} = \frac{E}{1-\nu^2} \begin{bmatrix} 1 & \nu \\ \nu & 1 \end{bmatrix} \begin{Bmatrix} \epsilon_r + \nu\sigma_3/E \\ \epsilon_\theta + \nu\sigma_3/E \end{Bmatrix}. \tag{3.50}$$

Next, the radial and circumferential strain components are expressed in terms of the radial displacement component with the help of eqs. (3.37a) and (3.37b) to find

$$\sigma_r - \frac{\nu\sigma_3}{1-\nu} = \frac{E}{1-\nu^2}(\epsilon_r + \nu\epsilon_\theta) = \frac{E}{1-\nu^2}\left(\frac{\mathrm{d}u_r}{\mathrm{d}r} + \frac{\nu u_r}{r}\right), \tag{3.51a}$$

$$\sigma_\theta - \frac{\nu\sigma_3}{1-\nu} = \frac{E}{1-\nu^2}(\epsilon_\theta + \nu\epsilon_r) = \frac{E}{1-\nu^2}\left(\frac{u_r}{r} + \nu\frac{\mathrm{d}u_r}{\mathrm{d}r}\right). \tag{3.51b}$$

Note that the circumferential displacement component, u_θ, vanishes for this problem featuring cylindrical symmetry.

Finally, the radial and circumferential stress components are introduced into the radial equilibrium equation (3.39a) to obtain a single equation for the radial displacement component

$$\frac{\mathrm{d}^2 u_r}{\mathrm{d}r^2} + \frac{1}{r}\frac{\mathrm{d}u_r}{\mathrm{d}r} - \frac{u_r}{r^2} = 0. \tag{3.52}$$

This is now an ordinary differential equation, similar to the Euler-Cauchy differential equation defined in eq. (3.43). It is, in fact, Navier's equation for this problem, and it could have been obtained by expressing eqs. (3.1) in polar coordinates, then imposing the cylindrical symmetry requirements.

Using the variable transformation $r = e^\xi$ and proceeding as before yields the displacement field as

$$u_r = C_1 r + C_2/r, \tag{3.53}$$

where C_1 and C_2 are two integration constants. The stress field, eqs. (3.51), becomes

$$\sigma_r - \frac{\nu\sigma_3}{1-\nu} = \frac{E}{1-\nu^2}\left[(1+\nu)C_1 - (1-\nu)\frac{C_2}{r^2}\right], \tag{3.54a}$$

$$\sigma_\theta - \frac{\nu\sigma_3}{1-\nu} = \frac{E}{1-\nu^2}\left[(1+\nu)C_1 + (1-\nu)\frac{C_2}{r^2}\right]. \tag{3.54b}$$

The integration constants are evaluated with the help of the boundary conditions at the inner and outer surfaces of the tube, $\sigma_r(r = R_e) = -p_e$ and $\sigma_r(r = R_i) = -p_i$, to find

$$\frac{EC_1}{1-\nu} = \frac{R_i^2 p_i - R_e^2 p_e}{R_e^2 - R_i^2} - \frac{\nu\sigma_3}{1-\nu}, \quad \text{and} \quad \frac{EC_2}{1+\nu} = \frac{(p_i - p_e)R_i^2 R_e^2}{R_e^2 - R_i^2}. \tag{3.55}$$

Introducing these constants into eqs. (3.54) yields the stress field as

$$\begin{aligned} \sigma_r(r) &= \frac{R_i^2 p_i - R_e^2 p_e}{R_e^2 - R_i^2} - \frac{1}{r^2}\frac{(p_i - p_e)R_i^2 R_e^2}{R_e^2 - R_i^2}, \\ \sigma_\theta(r) &= \frac{R_i^2 p_i - R_e^2 p_e}{R_e^2 - R_i^2} + \frac{1}{r^2}\frac{(p_i - p_e)R_i^2 R_e^2}{R_e^2 - R_i^2}. \end{aligned} \tag{3.56}$$

It is interesting to note that this stress field is identical to that found for the plane strain case, see eq. (3.47).

Note, however, that the axial displacements are different. Introducing the integration constants, eqs. (3.55), and the axial stress field, eq. (3.49), into eq. (3.53), yields

$$u_r = \frac{1-2\nu}{E}\frac{R_i^2 p_i - R_e^2 p_e}{R_e^2 - R_i^2} r + \frac{1+\nu}{E}\frac{(p_i - p_e) R_i^2 R_e^2}{R_e^2 - R_i^2}\frac{1}{r}. \tag{3.57}$$

This expression should be compared with the corresponding displacement field for the plane strain case, see eq. (3.48).

If no end caps are present, the cylinder is not pressurized and $\sigma_3 = 0$. The analysis presented in this example remains valid, and the stress distributions are still given by eq. (3.56) and the integration constants by eq. (3.55) with $\sigma_3 = 0$. Finally, the axial displacement field becomes

$$u_r = \frac{1-\nu}{E}\frac{R_i^2 p_i - R_e^2 p_e}{R_e^2 - R_i^2} r + \frac{1+\nu}{E}\frac{(p_i - p_e) R_i^2 R_e^2}{R_e^2 - R_i^2}\frac{1}{r}. \tag{3.58}$$

Example 3.4. Thin-walled tube in plane stress state

Consider the thin-walled tube of mean radius R_m and thickness t subjected to an internal pressure p_i, as depicted in fig. 3.10. This problem is the limiting case of example 3.3, where $R_i = R_m - t/2$ and $R_e = R_m + t/2$, with $t/R_m \ll 1$.

Due of the internal pressure, a hoop force N acts in the tube. The free body diagram of a unit length of the upper part of the tube shown in fig. 3.10 yields the following equilibrium equation for the forces acting in the vertical direction

$$2N = \int_0^\pi p_i R_m \sin\theta \, \mathrm{d}\theta = 2 p_i R_m, \tag{3.59}$$

or $N = p_i R_m$. For thin-walled tubes, it is reasonable to assume that the hoop stresses are uniformly distributed through the thickness of the wall, leading to $N = t\sigma_\theta$, where σ_θ the hoop stress. It then follows that

$$\sigma_\theta = \frac{R_m p_i}{t}. \tag{3.60}$$

It is easy to show that this hoop stress is the average of the distribution predicted by the more detailed solution derived in example 3.3 for a thick tube under the same conditions. Indeed, the average of the circumferential stress given in eq. (3.56) is

$$\bar{\sigma}_\theta = \frac{1}{t}\int_{R_i}^{R_e} \left[\frac{R_i^2 p_i - R_e^2 p_e}{R_e^2 - R_i^2} + \frac{1}{r^2}\frac{(p_i - p_e) R_i^2 R_e^2}{R_e^2 - R_i^2} \right] \mathrm{d}r = \frac{R_i p_i}{t}. \tag{3.61}$$

Since $R_m \approx R_i$ for thin-walled tubes, the two results are equivalent.

The hoop strain, ϵ_θ, is easily obtained as $\epsilon_\theta = \sigma_\theta / E = (R_m p_i)/(tE)$ and the radius of the ring increases by an amount $u_r = (R_m^2 p_i)/(Et)$, the radial displacement of the tube. Here again, this result can be checked by averaging the radial displacement distribution found earlier, see eq. (3.57), to find

$$\bar{u}_r = \frac{1}{t}\int_{R_i}^{R_e} u_r \,\mathrm{d}r = \frac{1-\nu}{Et}\frac{R_i^2 p_i}{2} + \frac{1+\nu}{Et}\frac{R_i^2 R_e^2 p_i}{R_e^2 - R_i^2}\ln\frac{R_e}{R_i}$$
$$\approx \frac{1-\nu}{Et}\frac{R_m^2 p_i}{2} + \frac{1+\nu}{Et}\frac{R_m^2 p_i}{2} = \frac{R_m^2 p_i}{Et}.$$

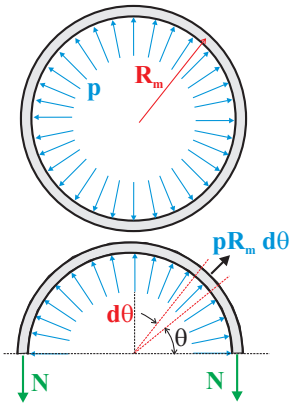

Fig. 3.10. Thin ring under internal pressure.

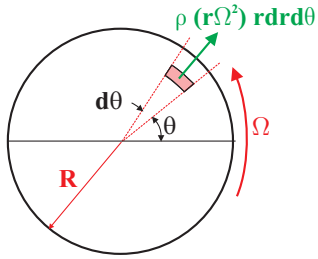

Fig. 3.11. Turbine disk rotating at high angular velocity Ω.

Example 3.5. Turbine disk at high angular velocity

Consider a homogeneous turbine disk of radius R rotating at high angular velocity Ω, as depicted in fig. 3.11. Due to the rotational speed of the turbine disk, each point on the disk is subjected to a centrifugal force $\rho(r\Omega^2)\, r\mathrm{d}r\mathrm{d}\theta$, where ρ is the material mass density, $-r\Omega^2$ the centripetal acceleration of the mass point, and $r\mathrm{d}r\mathrm{d}\theta$ the element of area on which the centrifugal force acts. Clearly, this centrifugal force acts in the radial direction of the polar coordinate system, and hence, the radial equilibrium equation, eq. (3.39a), must be modified to include a body force term,

$$\sigma_r - \sigma_\theta + r\frac{\mathrm{d}\sigma_r}{\mathrm{d}r} + \rho\Omega^2 r^2 = 0. \tag{3.62}$$

The disk is assumed to be in a state of plane stress, *i.e.*, $\sigma_3 = 0$, and the stresses can then be expressed in terms of the displacement field as

$$\sigma_r = \frac{E}{1-\nu^2}\left(\frac{\mathrm{d}u_r}{\mathrm{d}r} + \frac{\nu u_r}{r}\right), \quad \sigma_\theta = \frac{E}{1-\nu^2}\left(\frac{u_r}{r} + \nu\frac{\mathrm{d}u_r}{\mathrm{d}r}\right). \tag{3.63}$$

These expressions should be compared with eqs. (3.51).

Introducing the stress components, eq. (3.63), into the equilibrium equation of the problem, eq. (3.62), leads the governing equation for the radial displacement component

$$\frac{\mathrm{d}^2 u_r}{\mathrm{d}r^2} + \frac{1}{r}\frac{\mathrm{d}u_r}{\mathrm{d}r} - \frac{u_r}{r^2} + (1-\nu^2)\frac{\rho\Omega^2 r}{E} = 0. \tag{3.64}$$

The solution of this equation is

$$u_r = C_1 r + \frac{C_2}{r} - (1-\nu^2)\frac{\rho\Omega^2}{E}\frac{r^3}{8}, \tag{3.65}$$

where the first two terms represent the solution of the homogeneous equation and the last term is the particular solution associated with the nonhomogeneous term in the equation. The displacement at the center of the disk, *i.e.*, at $r = 0$, must remain finite, and hence, $C_2 = 0$. The remaining integration constant, C_1, is determined by the boundary condition $\sigma_r(r = 0) = 0$ to give

$$C_1 = \frac{3+\nu}{8(1+\nu)}(1-\nu^2)\frac{\rho\Omega^2}{E}R^2. \tag{3.66}$$

The stress field then becomes

$$\frac{\sigma_r}{\rho R^2\Omega^2} = \frac{3+\nu}{8}(1-\bar{r}^2), \quad \frac{\sigma_\theta}{\rho R^2\Omega^2} = \frac{3+\nu}{8}\left(1 - \frac{1+3\nu}{3+\nu}\bar{r}^2\right), \tag{3.67}$$

where $\bar{r} = r/R$. Note that the maximum stresses are found at the center of the disk, where $\sigma_r/(\rho R^2\Omega^2) = \sigma_\theta/(\rho R^2\Omega^2) = (3+\nu)/8$. According to von Mises' criterion, the equivalent stress at that point becomes $\sigma_{eq}/(\rho R^2\Omega^2) = (3+\nu)/8$. The disk yields when $\sigma_{eq} = \sigma_y$, where σ_y is the material yield stress. The maximum speed at which the disk can rotate before centrifugal forces induce yielding is then

$$\Omega = \sqrt{\frac{8\sigma_y}{(3+\nu)\rho R^2}}. \tag{3.68}$$

Example 3.6. Thin sheet with hole under uniaxial stress

Consider a thin sheet of material featuring a small hole. This problem is an idealization of a frequently encountered situation in aircraft structures. For instance, holes or cutout are common occurrences in aircraft skins to make a place for bolts, rivets, windows or access covers; similarly, bulkheads may have many holes that are passageways for cables, wires, or hydraulic lines. If the thin sheet is subjected to in-plane loading, a plane stress distribution will develop in the skin. Intuitively, the presence of the hole will increase the stress level in the sheet as compared to the stress level in the absence of a hole. The hole is said to be a *stress riser or stress concentrator*. This example will evaluate the stress distribution around the hole to identify the maximum stress level. The ratio of this maximum stress level to that observed in the absence of a hole is called the *stress concentration factor*.

Figure 3.12 shows the configuration considered here. A square plate of side dimension b presents a central circular hole of radius R_i, such that $R_i/b \ll 1$. The sheet is subjected to a far field unidirectional stress σ_a. A Cartesian coordinate system is selected with its origin at the center of the hole and axis $\bar{\imath}_2$ is aligned with the direction of the applied stress, σ_a. Since the hole is circular, it is natural to also

make use of a polar coordinate system with its origin at the center of the hole; as shown in fig. 3.12, angle θ is measured from axis $\bar{\imath}_1$. Clearly, this problem does not present the cylindrical symmetry of the previous examples. It will be shown, however, that the problem can be treated as the superposition of two simpler problems: an axisymmetric and a non-axisymmetric problem.

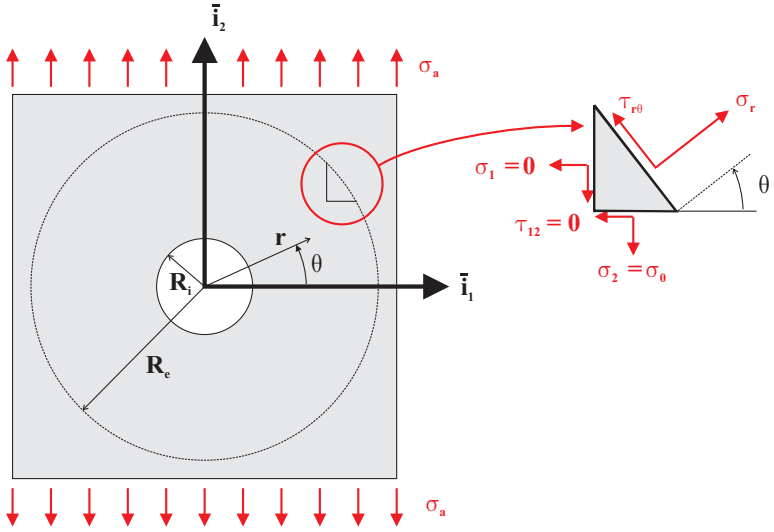

Fig. 3.12. Thin sheet with central hole of radius R_i subjected to uniaxial stress $\sigma_2 = \sigma_a$; also shown is the far field circle at $r = R_e$ where boundary conditions are applied.

The sheet is in a state of plane stress, and in the absence of body forces, the governing equation for Airy's stress function is the homogeneous form of the biharmonic partial differential equation (3.29). The boundary conditions around the edge of the hole are easily expressed in polar coordinates: both radial and shear stress components must vanish, $\sigma_r(r = R_i) = 0$ and $\tau_{r\theta}(r = R_i) = 0$. Because the circumferential stress, σ_θ, is not exposed around the inner edge of the circle, no condition is imposed on this stress component.

To avoid specifying boundary conditions in the Cartesian coordinate system, the far field stress σ_a is assumed to act on a circle of radius $R_e \gg R_i$; this assumption is consistent with the fact that the dimensions of the plate are much larger than the radius of the hole, $b \gg R_i$, as stated before. This implies $\sigma_1(r = R_e) = 0$, $\sigma_2(r = R_e) = \sigma_a$ and $\tau_{12}(r = R_e) = 0$.

These boundary conditions are stated in an awkward manner: stress components in a Cartesian system, σ_1, σ_2 and τ_{12}, are given at locations specified by polar coordinates $r = R_e$ and angle θ is arbitrary. To resolve this discrepancy, the stress components in the Cartesian system are transformed to their polar counterparts using the formulas for the rotation of stress components, eqs. (1.49a) and (1.49c), to

find

$$\sigma_r(r=R_e,\theta)=\frac{\sigma_1+\sigma_2}{2}+\frac{\sigma_1-\sigma_2}{2}\cos 2\theta+\tau_{12}\sin 2\theta=\frac{\sigma_a}{2}-\frac{\sigma_a}{2}\cos 2\theta,$$
$$\tau_{r\theta}(r=R_e,\theta)=-\frac{\sigma_1-\sigma_2}{2}\sin 2\theta+\tau_{12}\cos 2\theta=\frac{\sigma_a}{2}\sin 2\theta. \tag{3.69}$$

These equations could also be obtained directly from a Mohr's circle visualization, or they could be developed directly by expressing the equilibrium conditions of the triangular differential element depicted in the right portion of fig. 3.12.

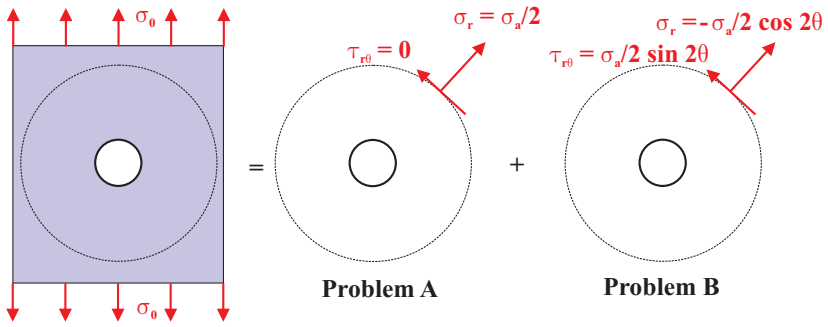

Fig. 3.13. The solution of the desired problem is found by superposing the solutions of two simpler problems: an axisymmetric problem, denoted "problem A" and a non-axisymmetric problem, denoted "problem B".

It now becomes possible to split the original problem into two simpler problems, both expressed in terms of polar coordinates as illustrated in fig. 3.13.

1. The axisymmetric problem, denoted Problem A, is subjected to the following boundary conditions: $\sigma_r = \tau_{r\theta} = 0$ around the edge of the hole, *i.e.*, at $r = R_i$, and $\sigma_r = \sigma_a/2$ and $\tau_{r\theta} = 0$ around the far field circular boundary, *i.e.*, at $r = R_e$. This problem is axisymmetric because the geometry of the problem presents cylindrical symmetry and the boundary conditions are independent of θ.
2. The non-axisymmetric problem, denoted Problem B, is subjected to the following boundary conditions $\sigma_r = \tau_{r\theta} = 0$ around the edge of the hole, *i.e.*, for $r = R_i$, and $\sigma_r = -\sigma_a/2\ \cos 2\theta$ and $\tau_{r\theta} = \sigma_a/2\ \sin 2\theta$ around the far field circular boundary, *i.e.*, for $r = R_e$. This problem is not axisymmetric because while the geometry of the problem does present cylindrical symmetry, the boundary conditions do depend on θ.

The solution to Problem A is developed in example 3.3. It consists of a thin cylinder subjected to an external pressure, $p_e = -\sigma_a/2$. The stress field is readily obtained by introducing $p_i = 0$ and $p_e = -\sigma_a/2$ eqs. (3.47) to find

$$\sigma_r^A = \frac{\sigma_a}{2}\left[\frac{R_e^2}{R_e^2 - R_i^2} - \frac{R_i^2 R_e^2}{R_e^2 - R_i^2}\frac{1}{r^2}\right],\ \sigma_\theta^A = \frac{\sigma_a}{2}\left[\frac{R_e^2}{R_e^2 - R_i^2} + \frac{R_i^2 R_e^2}{R_e^2 - R_i^2}\frac{1}{r^2}\right]. \tag{3.70}$$

The solution of Problem B is more difficult, and requires the solution of the homogeneous bi-harmonic equation in polar coordinates given by eq. (3.41). Since the bi-harmonic operator only contains even derivatives with respect to θ, an approach based on separation of variables seems appropriate. A solution of the following form is proposed

$$\phi(r,\theta) = \eta(r)\cos 2\theta. \tag{3.71}$$

Substituting this assumed solution into the homogeneous bi-harmonic equation in polar coordinates, eq. (3.41), leads to the following equation for Airy's stress function

$$\nabla^4\phi = \left(\frac{\mathrm{d}^4\eta}{\mathrm{d}r^4} + \frac{2}{r}\frac{\mathrm{d}^3\eta}{\mathrm{d}r^3} - \frac{9}{r^2}\frac{\mathrm{d}^2\eta}{\mathrm{d}r^2} + \frac{9}{r^3}\frac{\mathrm{d}\eta}{\mathrm{d}r}\right)\cos 2\theta = 0.$$

Because this expression must be valid for *all values* θ, the term in parentheses must vanish, and hence,

$$\frac{\mathrm{d}^4\eta}{\mathrm{d}r^4} + \frac{2}{r}\frac{\mathrm{d}^3\eta}{\mathrm{d}r^3} - \frac{9}{r^2}\frac{\mathrm{d}^2\eta}{\mathrm{d}r^2} + \frac{9}{r^3}\frac{\mathrm{d}\eta}{\mathrm{d}r} = 0.$$

This is another instance of the Euler-Cauchy differential equation first encountered in section 3.5. Using the same procedure as before, the following solution is found: $\eta(r) = C_1 + C_2 r^2 + C_3 r^4 + C_4/r^2$. Airy's stress function now becomes

$$\phi(r,\theta) = \left[C_1 + C_2 r^2 + C_3 r^4 + \frac{C_4}{r^2}\right]\cos 2\theta.$$

Next, the stress field is obtained by introducing the stress function into eqs.(3.38) to find the stress components as

$$\begin{aligned}
\sigma_r &= \frac{1}{r}\frac{\partial\phi}{\partial r} + \frac{1}{r^2}\frac{\partial^2\phi}{\partial\theta^2} = -\left[2C_2 + \frac{4C_1}{r^2} + \frac{6C_4}{r^4}\right]\cos 2\theta,\\
\sigma_\theta &= \frac{\partial^2\phi}{\partial r^2} = \left[2C_2 r + 12C_3 r^2 + \frac{6C_4}{r^4}\right]\cos 2\theta,\\
\tau_{r\theta} &= \frac{1}{r^2}\frac{\partial\phi}{\partial\theta} - \frac{1}{r}\frac{\partial^2\phi}{\partial r\partial\theta} = \left[2C_2 + 6C_3 r^2 - \frac{2C_1}{r^2} - \frac{6C_4}{r^4}\right]\sin 2\theta.
\end{aligned}$$

The boundary conditions, $\sigma_r = 0$ and $\tau_{r\theta} = 0$ at $r = R_i$, yield the following two equations

$$\begin{aligned}
\sigma_r(r = R_i) &= -\left[\frac{4}{R_i^2}C_1 + 2C_2 + \frac{6C_4}{R_i^4}\right]\cos 2\theta = 0,\\
\tau_{r\theta}(r = R_i) &= \left[-\frac{2}{R_i^2}C_1 + 2C_2 + 6R_i^2 C_3 - \frac{6C_4}{R_i^4}\right]\cos 2\theta = 0,
\end{aligned}$$

whereas the boundary conditions, $\sigma_r = -\sigma_a/2\ \cos 2\theta$ and $\tau_{r\theta} = \sigma_a/2\ \sin 2\theta$ at $r = R_e$, lead to

$$\sigma_r(r=R_e) = -\left[\frac{4}{R_e^2}C_1 + 2C_2 + \frac{6C_4}{R_e^4}\right]\cos 2\theta = -\frac{\sigma_a}{2}\cos 2\theta,$$
$$\tau_{r\theta}(r=R_e) = \left[-\frac{2}{R_e^2}C_1 + 2C_2 + 6R_e^2C_3 - \frac{6C_4}{R_e^4}\right]\sin 2\theta = \frac{\sigma_a}{2}\sin 2\theta.$$

These four algebraic equations are used to determine the four integration constants, C_1, C_2, C_3 and C_4. This task is more easily achieved by recasting the equations in a matrix form as

$$\begin{bmatrix} -4/R_i^2 & -2 & 0 & -6/R_i^4 \\ -2/R_i^2 & 2 & 6R_i^2 & -6/R_i^4 \\ 4/R_e^2 & 2 & 0 & 6/R_e^4 \\ -2/R_e^2 & 2 & 6R_e^2 & -6/R_e^4 \end{bmatrix} \begin{Bmatrix} C_1 \\ C_2 \\ C_3 \\ C_4 \end{Bmatrix} = \begin{Bmatrix} 0 \\ 0 \\ \sigma_a/2 \\ \sigma_a/2 \end{Bmatrix}. \tag{3.72}$$

Note that the canceling of the trigonometric function of angle θ indicates that the assumed form of Airy's stress function, eq. (3.71), is able to satisfy all the boundary conditions for the particular problem. The solution to this set of algebraic equations is readily accomplished, but results are long and tedious expressions.

Since the interest is not in solutions for finite values of the outer radius, R_e, it is easier to immediately consider the situation where $R_e \to \infty$, or more specifically, where $1/R_e \to 0$. Applying this to eq. (3.72) results in

$$\begin{bmatrix} -4/R_i^2 & -2 & 0 & -6/R_i^4 \\ -2/R_i^2 & 2 & 6R_i^2 & -6/R_i^4 \\ 0 & 2 & 0 & 0 \\ 0 & 0 & 6 & 0 \end{bmatrix} \begin{Bmatrix} C_1 \\ C_2 \\ C_3 \\ C_4 \end{Bmatrix} = \begin{Bmatrix} 0 \\ 0 \\ \sigma_a/2 \\ 0 \end{Bmatrix}.$$

The last equation is divided by R_e^2 before taking the limit to insure that the third term remained finite. These equations can be solved to yield

$$C_1 = -\frac{R_i^2}{2}\sigma_a, \quad C_2 = \frac{\sigma_a}{4}, \quad C_3 = 0, \quad C_4 = \frac{R_i^4}{4}\sigma_a.$$

The solutions to Problem A and Problem B can now be combined to yield the complete solution for the state of stress around the circular hole of radius R_i

$$\sigma_r(r,\theta) = \frac{\sigma_a}{2}\left[\left(1 - \frac{R_i^2}{r^2}\right) + \left(-1 + 4\frac{R_i^2}{r^2} - 3\frac{R_i^4}{r^4}\right)\cos 2\theta\right],$$
$$\sigma_\theta(r,\theta) = \frac{\sigma_a}{2}\left[\left(1 + \frac{R_i^2}{r^2}\right) + \left(1 + 3\frac{R_i^4}{r^4}\right)\cos 2\theta\right],$$
$$\tau_{r\theta}(r,\theta) = \frac{\sigma_a}{2}\left[1 + 2\frac{R_i^2}{r^2} - 3\frac{R_i^4}{r^4}\right]\sin 2\theta.$$

These results show that the stress components decrease in the inverse proportion of the square of the distance from the center of the hole. As expected, at a large distance from the hole, the far field uniaxial stress state is recovered, $\sigma_r = \sigma_a/2\,(1 - \cos 2\theta)$,

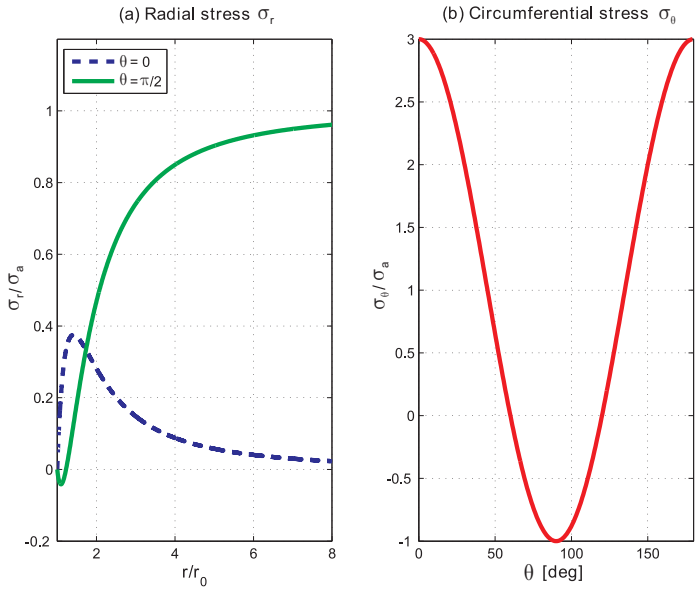

Fig. 3.14. Plots of stress state around circular hole in a thin sheet: (a) σ_r/σ_a along radii at $\theta = 0$ and $\theta = \pi/2$, and (b) σ_θ/σ_a around inside edge of hole.

$\sigma_\theta = \sigma_a\ (1 + \cos 2\theta)$, and $\tau_{r\theta} = \sigma_a/2\ \sin 2\theta$, which in the Cartesian coordinate system, corresponds to $\sigma_2 = \sigma_a$ and $\sigma_1 = \tau_{12} = 0$. Figure 3.14(a) shows that the radial stress component, σ_r, rapidly approaches its asymptotic values of zero and σ_a, along two radial lines corresponding to $\theta = 0$ and 90 degrees, respectively.

Around the edge of the hole, *i.e.*, for $r = R_i$, the radial and shear stress components vanish, as required, but the circumferential stress does not: $\sigma_\theta(\theta) = \sigma_a(1+2\cos 2\theta)$. Figure 3.14(b) shows the distribution of this hoop stress around the hole; note the peak values of $3\sigma_a$ at $\theta = 0$ or π, and of $-\sigma_a$ at $\theta = \pi/2$ or $3\pi/2$. The distribution of hoop stress over the other half of the hole, *i.e.*, for $\pi \leq \theta \leq 2\pi$, is the mirror image of that on the upper half of the hole.

Several important conclusions can be drawn from this example. The most significant is that the presence of a circular hole in a thin sheet under a uniaxial state of stress causes the appearance of a peak circumferential stress at the edge of the hole. This stress component peaks at a level that is 3 times as large as that of the applied stress, *i.e.*, the hole creates a *stress concentration factor* of 3. If the sheet is designed based on a simple yield criterion, $\sigma_{\max} < \sigma_y$, where σ_y is the yield stress for the material, the presence of the hole reduces the load carrying capacity of the sheet by a factor of three. The stress concentration factor is *independent of the hole size*; the above analysis just requires the hole diameter to be much smaller than the dimensions of the sheet. Consequently, no matter how small the hole is, the load carrying capability of the panel is reduced by a factor of three. In practice, because the

hoop stress peaks in a relatively small region, the material will locally yield, and the load carrying capacity of the sheet will not be reduced as dramatically. If the panel is subjected to cyclic loads, however, cracks are likely to develop in the high stress area, possibly reducing the life of the component significantly.

The disturbance in the far field stress caused by the presence of the hole quickly decays away from the center of the hole, as illustrated in fig. 3.14. This means that the presence of the hole in "felt" only in a small area. Finally, it is interesting to note that the hoop stress is actually negative, $\sigma_\theta = -\sigma_a$, in the area around $\theta = \pm\pi/2$, that is, in the regions above and below the hole along axis $\bar{\imath}_2$. Consequently, secondary attachments might be made in this area without causing further problems.

The solution presented above is readily generalized to the case where $\sigma_1 = \sigma_b$ and $\sigma_2 = 0$, simply by replacing σ_a by σ_b and θ by $\theta + \pi/2$ in the above solution. Indeed, in the above solution, the applied loading direction is arbitrarily selected to coincide with that of axis $\bar{\imath}_2$. The solution for a sheet subjected to the biaxial state of stress $\sigma_1 = \sigma_b$ and $\sigma_2 = \sigma_a$ would then be obtained by superposing the two solutions. For example, if the far field stress is the pure shear stress state, the solution is obtained by setting $\sigma_1 = -\tau_0$ and $\sigma_2 = \tau_0$.

Example 3.7. Reinforced hole in a thin panel

In example 3.6, the presence of a hole in a thin panel is shown to cause a considerable disturbance in the stress field in the panel, and a stress concentration factor appears around the edge of the hole. In this example, the following question is raised: is it possible to eliminate this stress concentration by reinforcing the edge of the hole? Figure 3.15 shows the configuration to be investigated: the panel features a hole of radius R_i, but this time, a circular ring of cross-sectional area $\mathcal{A}$ and thickness t reinforces the hole. The circular ring that reinforces the hole is called a "boss."

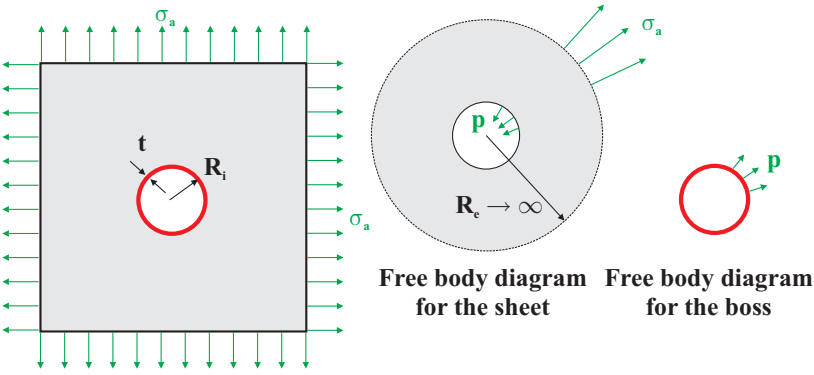

Fig. 3.15. A thin panel with a hole subjected to a biaxial state of stress.

The panel is subjected to a biaxial state of stress, $\sigma_1 = \sigma_2 = \sigma_a$. Furthermore, the dimensions of the panel are assumed to be much larger than the radius of the

hole. Consequently, the square panel can be replaced by a circular panel of radius $R_e \to \infty$, subjected to an external pressure, $p_e = -\sigma_a$. Finally, the boss fits into the circular hole, and hence, the boss and panel must interact through an unknown pressure p. Figure 3.15 shows the free body diagram of the panel and boss, separately. The circular panel is subjected to an external pressure, $p_e = -\sigma_a$, and an internal pressure, $p_i = -p$, of unknown magnitude. On the other hand, the boss is a thin ring subjected to an internal pressure of magnitude p. The magnitude of this unknown pressure will be found by imposing displacement compatibility: the radial displacements of the boss and hole in which it fits must match.

Because the circular panel is in a state of plane stress, the results developed in example 3.3 do apply. In particular, the stress field in the panel is given by eqs. (3.56), and hence $\sigma_r = -p_e - (p_i - p_e)/\bar{r}^2$ and $\sigma_\theta = -p_e + (p_i - p_e)/\bar{r}^2$, where $\bar{r} = r/R_i$. In this case, $p_e = -\sigma_a$ and $p_i = -p$, leading to the following stress field in the panel

$$\sigma_r = \sigma_a - \frac{\sigma_a - p}{\bar{r}^2}, \quad \sigma_\theta = \sigma_a + \frac{\sigma_a - p}{\bar{r}^2}. \tag{3.73}$$

Next, the radial displacement distribution follows from eq. (3.58) as $Eu_r/R_i = -(1-\nu)p_e\bar{r} + (1+\nu)(p_i - p_e)/\bar{r}$. Because, $p_e = -\sigma_a$ and $p_i = -p$, the radial displacement of the edge of the hole becomes

$$u_r(r = R_i) = \frac{R_i}{E}\left[(1-\nu)\sigma_a + (1+\nu)(\sigma_a - p)\right] = \frac{R_i}{E}\left[2\sigma_a - (1+\nu)p\right].$$

On the other hand, the radial displacement of the boss is evaluated with the help of eq. (3.62) to find $u_r = (R_i^2 p)/(Et)$. If w is the width of the boss, its cross-sectional area is then $\mathcal{A} = wt$, and the radial displacement becomes $u_r = (R_i^2 wp)/(E\mathcal{A})$. Compatibility requires the radial displacement of the hole in the sheet to be identical to that of the boss, *i.e.*, $R_i\left[2\sigma_a - (1+\nu)p\right]/E = (R_i^2 wp)/(E\mathcal{A})$. This condition yields the interface pressure between the boss and sheet as

$$p = \frac{2\sigma_a}{(1+\nu) + R_i w/\mathcal{A}}. \tag{3.74}$$

The stress field in the panel is evaluated by introducing the value of this pressure into eqs. (3.73).

It is now possible to answer the question raised at the beginning of this example: is it possible to eliminate this stress concentration by reinforcing the edge of the hole with the boss? A cursory examination of eq. (3.73) reveals that if $p = \sigma_a$, the stress components in the panel are $\sigma_r = \sigma_\theta = \sigma_a$, *i.e.*, the stress field is *identical as that in the panel without a hole*. If $p = \sigma_a$, eq. (3.74) then implies

$$\mathcal{A} = \frac{wR_i}{1-\nu}. \tag{3.75}$$

In other words, if the cross-sectional area of the boss is given by the above relationship, the stress field in the panel is undisturbed by the presence of the hole: the panel "does not see" or "does not feel" the presence of the hole. A similar technique is

used in aircraft fuselages: a boss is placed around the windows of the fuselage so as to leave the stress field undisturbed to the largest possible extent. Of course, since the fuselage is subjected to a variety of loading conditions, the boss minimizes the effect of the window on the fuselage stress distribution without completely eliminating it.

Example 3.8. Thin-walled spherical pressure vessel

The reasoning developed in example 3.4 can readily be extended to the situation of a thin-walled sphere of radius R and thickness t subjected to an internal pressure p, as shown in fig. 3.16. This type of configuration is representative of spherical pressure vessels.

First, the sphere is cut by a horizontal plane passing through its center, to reveal the free body diagram shown in the figure. Due to the symmetry of the problem, the pressure acting on the upper half of the sphere will be equilibrated by a hoop stress, σ_h, which is uniformly distributed around the circle at the intersection of the sphere with the plane of the cut. The total upward force generated by the pressure, $\pi R^2 p$, is equilibrated by the downward force generated by the distributed hoop stress, $2\pi R t \sigma_h$, assumed to be uniformly distributed through the thickness of the wall. This yields the following result

$$\sigma_h = \frac{pR}{2t}. \tag{3.76}$$

Note that the hoop stress is half of that in a pressurized tube of equal radius and thickness, see eq. (3.76).

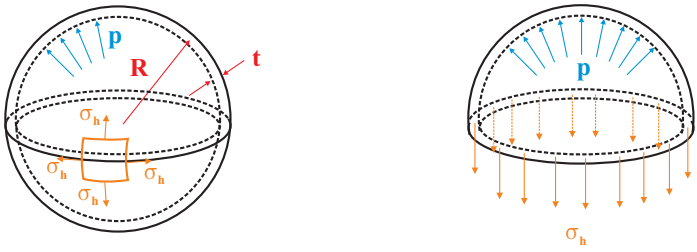

Fig. 3.16. Thin sphere under internal pressure.

Of course, in view of the spherical symmetry of the problem, the orientation of the plane of the cut is arbitrary. Hence, the hoop stress derived above is acting on a face with an arbitrary orientation. As shown in fig. 3.16, the stresses acting on an arbitrary differential element cut from the thin-walled sphere are σ_h in two orthogonal directions. Because the shear stress component vanishes, these are the principal stresses, and hence, $\sigma_{p1} = \sigma_{p2} = \sigma_h$. Note that Mohr's circle then reduces to a single point at ordinate σ_h.

For a linearly elastic material, the hoop strain, ϵ_h, is obtained from Hooke's law, eq. (2.4), as

$$\epsilon_1 = \epsilon_2 = \epsilon_h = \frac{1-\nu}{2}\frac{R}{t}\frac{p}{E}. \tag{3.77}$$

The deformation is identical in all directions, due to the spherical symmetry of the problem. Since the shear strain components vanish, the principal strains are $\epsilon_{p1} = \epsilon_{p2} = \epsilon_h$. The radius of the sphere increases by an amount $\Delta R = (1-\nu)(pR^2)/(2Et)$.

If the wall thickness is very much smaller than the radius of the sphere, its curvature become unimportant. Hence, it is possible to look at the sphere as a thin, flat sheet of material subjected to a biaxial state of stress where $\sigma_a = \sigma_h$, as depicted in fig. 3.15.

Pressure vessels must often be drilled to install manifolds that monitor the internal pressure or to let the pressurized gas or fluid in and out of the vessel. Such situation is identical to that discussed in example 3.7: a thin panel under a biaxial state of stress featuring a circular hole. To minimize the effect of the hole on the stress distribution in the pressure vessel, it is common to reinforce the hole with a circular ring, as discussed in the example. For the optimum boss design given by eq. (3.75), the stress distribution in the spherical pressure vessel will remain undisturbed by the presence of a circular hole.

3.5.1 Problems

Problem 3.1. Navier's equations
Develop the three Navier equations following the procedure described in section 3.1.1.

Problem 3.2. A solution to Navier's equations
In principle, Navier's equations should allow solution for the unknown displacements within a solid body from which the stresses can be computed using the strain-displacement and stress-strain equations. However, they are not as useful as expected because it is very difficult to express the necessary displacement boundary conditions for most practical problems. Nonetheless a few solutions can be illustrated. Consider a problem with body forces given by: $b_1 = -6Gx_2x_3$, $b_2 = 2Gx_3x_1$, and $b_3 = 10Gx_1x_2$, and assume displacements given by $u_1 = C_1x_1^2x_2x_3$, $u_2 = C_2x_1x_2^2x_3$, and $u_3 = C_3x_1x_2x_3^2$. Also assume $G = E/2(1+\nu)$ and ν = 1/4. Determine the constants, C_1, C_2, and C_3 which allow satisfaction of the Navier equations. Hint: you will eventually need to solve 3 simultaneous equations.

Problem 3.3. Equilibrium equations in polar coordinates
Derive the plane stress equilibrium equations (one equation in the r and a second in the θ directions). Figure 3.6 provides the appropriate free body diagram. Make sure when you write a force equilibrium equation that you multiply all stresses by appropriate areas (assume the material has a unit thickness). You will need to account for the slight difference ($\mathrm{d}\theta$) in the direction of on opposite sides of the element when writing the equilibrium equations in both the r and θ directions. You will also need to use Taylor Series to express the differential changes in σ_r and σ_θ in the same manner as is done for rectangular differential areas.

Problem 3.4. Strain compatibility equations in polar coordinates
For plane stress problems presenting cylindrical symmetry, the strain-displacement equations expressed in polar coordinates are: $\epsilon_r = \mathrm{d}u_r/\mathrm{d}r$, $\epsilon_\theta = u_r/r$, and $\gamma_{r\theta} = 0$. *(1)* How many strain compatibility equations exist for this problem? *(2)* Derive the strain compatibility equations, if any.

Problem 3.5. Thick-walled cylinder under internal pressure
Consider a thick-walled cylinder of internal and external radii R_i and R_e, respectively, in a state of plane strain subjected to an internal pressure p_i. *(1)* Plot the non-dimensional radial stress, σ_r/p_i, distribution through the thickness of the cylinder. *(2)* Plot the distribution of non-dimensional circumferential stress, σ_θ/p_i. *(3)* Plot the distribution of von Mises' equivalent stress, σ_e/p_i. *(4)* If the yield stress for the material is σ_y, plot the maximum internal pressure the thick-walled cylinder can carry as a function of $\rho = R_e/R_i$. What is the maximum pressure p_i/σ_y that can be carried by a very thick cylinder? *(5)* Plot the distribution of non-dimensional radial strain, $E\epsilon_r/p_i$. *(6)* Plot the distribution of non-dimensional circumferential strain, $E\epsilon_\theta/p_i$. *(7)* Plot the distribution of non-dimensional radial displacement, $Eu_r/(R_i p_i)$. Present all your results for $\rho = 1.5, 2.0$ and 3.0; use the radial coordinate $\bar{r} = r/R_i$.

Problem 3.6. Thick-walled cylinder under external pressure
Consider a thick-walled cylinder of internal and external radii R_i and R_e, respectively, in a state of plane strain subjected to an external pressure p_e. *(1)* Plot the non-dimensional radial stress, σ_r/p_e, distribution through the thickness of the cylinder. *(2)* Plot the distribution of non-dimensional circumferential stress, σ_θ/p_e. *(3)* Plot the distribution of von Mises' equivalent stress, σ_e/p_e. *(4)* If the yield stress for the material is σ_y, plot the maximum external pressure the thick-walled cylinder can carry as a function of $\rho = R_e/R_i$. What is the maximum pressure p_e/σ_y that can be carried by a very thick cylinder? *(5)* Plot the distribution of non-dimensional radial strain, $E\epsilon_r/p_e$. *(6)* Plot the distribution of non-dimensional circumferential strain, $E\epsilon_\theta/p_e$. *(7)* Plot the distribution of non-dimensional radial displacement, $Eu_r/(R_i p_e)$. Present all your results for $\rho = 1.5, 2.0$ and 3.0; use the radial coordinate $\bar{r} = r/R_i$.

Problem 3.7. Thick-walled cylinder under internal pressure
Consider a thick-walled cylinder of internal and external radii R_i and R_e, respectively, in a state of plane stress subjected to an internal pressure p_i. *(1)* Plot the non-dimensional radial stress, σ_r/p_i, distribution through the thickness of the cylinder. *(2)* Plot the distribution of non-dimensional circumferential stress, σ_θ/p_i. *(3)* Plot the distribution of von Mises' equivalent stress, σ_e/p_i. *(4)* If the yield stress for the material is σ_y, plot the maximum internal pressure the thick-walled cylinder can carry as a function of $\rho = R_e/R_i$. What is the maximum pressure p_i/σ_y that can be carried by a very thick cylinder? *(5)* Plot the distribution of non-dimensional radial strain, $E\epsilon_r/p_i$. *(6)* Plot the distribution of non-dimensional circumferential strain, $E\epsilon_\theta/p_i$. *(7)* Plot the distribution of non-dimensional radial displacement, $Eu_r/(R_i p_i)$. Present all your results for $\rho = 1.5, 2.0$ and 3.0; use the radial coordinate $\bar{r} = r/R_i$.

Problem 3.8. Thick-walled cylinder under external pressure
Consider a thick-walled cylinder of internal and external radii R_i and R_e, respectively, in a state of plane stress subjected to an external pressure p_e. *(1)* Plot the non-dimensional radial stress, σ_r/p_e, distribution through the thickness of the cylinder. *(2)* Plot the distribution of non-dimensional circumferential stress, σ_θ/p_e. *(3)* Plot the distribution of von Mises' equivalent stress, σ_e/p_e. *(4)* If the yield stress for the material is σ_y, plot the maximum external pressure the thick-walled cylinder can carry as a function of $\rho = R_e/R_i$. What is the maximum pressure p_e/σ_y that can be carried by a very thick cylinder? *(5)* Plot the distribution of non-dimensional radial strain, $E\epsilon_r/p_e$. *(6)* Plot the distribution of non-dimensional circumferential strain, $E\epsilon_\theta/p_e$. *(7)* Plot the distribution of non-dimensional radial displacement, $Eu_r/(R_i p_e)$. Present all your results for $\rho = 1.5, 2.0$ and 3.0; use the radial coordinate $\bar{r} = r/R_i$.

Problem 3.9. Disk rotating at high speed

A disk of mass density ρ, and inner and outer radii denoted a and b, respectively, is spinning about a fixed point at an angular velocity Ω. *(1)* Plot the distribution of non-dimensional radial stress, $\sigma_r/(\rho a^2\Omega^2)$, through the thickness of the disk. *(2)* Plot the distribution of non-dimensional circumferential stress, $\sigma_\theta/(\rho a^2\Omega^2)$. *(3)* Plot the distribution of non-dimensional von Mises' equivalent stress, $\sigma_e/(\rho a^2\Omega^2)$. Present your stress distributions for $b/a = 1.5$, 2.0 and 3.0, as a function of $\bar{r} = r/a$. *(4)* First, let the inner radius, a, be fixed. Plot the maximum allowable non-dimensional angular speed, $\Omega_{\max}\sqrt{\rho a^2/\sigma_y}$ as a function of $b/a \in [1.0, 10.0]$, *i.e.*, as the outer radius of the cylinder increases. Use von Mises' criterion to predict yielding, σ_y denotes the yield stress. *(5)* Next, let the outer radius, b, be fixed. Plot the maximum allowable non-dimensional angular speed, $\Omega_{\max}\sqrt{\rho b^2/\sigma_y}$ as a function of $a/b \in [0.0, 1.0]$, *i.e.*, as the inner radius of the cylinder decreases. Comment on the significance of these last two results. Hint: the boundary conditions of the problem are $\sigma_r(r = a) = 0$ and $\sigma_r(r = b) = 0$.

Problem 3.10. Two cylinder assembly

Figure 3.17 shows two cylinders that have been assembled by a process called "shrink-fitting." The inner cylinder has nominal internal and external radii of a and b, respectively, whereas the corresponding quantities for the external cylinder are b and c, respectively. Assume that the unconstrained external radius of the inner cylinder *exceeds* the initially unconstrained internal radius of the external cylinder by an amount δ, where $\delta \ll b$. The two components are assembled by first heating the outer cylinder so that it expands, slipping the outer cylinder over the inner, then letting the two components cool down. *(1)* Find the pressure, p, acting between the two cylinder after cool down. *(2)* Find the common radial displacement of the two cylinder at their interface. Hint: draw a free body diagram of the two cylinders separately. The internal cylinder is acted upon by an external pressure, p, whereas the external cylinder carries an internal pressure, p. This pressure can be found by imposing the compatibility of radial displacement at the interface between the cylinders.

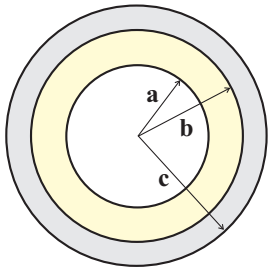

Fig. 3.17. Two concentric cylinder assembled by heat treatment.

Problem 3.11. Von Mises' equivalent stress around a hole in thin sheet

Consider a thin panel with a central circular hole of radius R_i subjected to a far field biaxial state of stress $\sigma_1 = \sigma_b$ and $\sigma_2 = \sigma_a$. *(1)* Evaluate the stress field in the panel. *(2)* Evaluate the non-dimensional Von Mises' equivalent stress $\sigma_{\rm eq}/\sigma_a$, where $\sigma_{\rm eq}$ is defined by eq. (2.36). *(3)* Plot the distribution of the equivalent stress for $1 \leq \bar{r} \leq 5$, where $\bar{r} = r/R_i$, and $0 \leq \theta \leq 2\pi$. Plot your results for $\sigma_b/\sigma_a =$ - 1.0, *i.e.*, when the panel is in a state of pure shear, and for $\sigma_b/\sigma_a = 1.0$. *(4)* What are the stress concentration factors in each case? Note: use a software package to generate the three dimensional plots.